Published in final edited form as:
J Proteome Res. 2009 July ; 8(7): 3497–3511. doi:10.1021/pr9001614.

Proteomic Studies of Nitrated Alpha-Synuclein Microglia Regulation by CD4+CD25+ T Cells

Ashley D. Reynolds[1], **David K. Stone**[1], **R. Lee Mosley**[1], and **Howard E. Gendelman**[1,2,*]

Ashley D. Reynolds: areynold@unmc.edu; David K. Stone: dstone@unmc.edu; R. Lee Mosley: rlmosley@unmc.edu; Howard E. Gendelman: hegendel@unmc.edu

[1]Department of Pharmacology and Experimental Neuroscience, University of Nebraska Medical Center, Omaha, Nebraska 68198-5800, USA

[2]Department of Internal Medicine, University of Nebraska Medical Center, Omaha, Nebraska 68198-5800, USA

Abstract

Microglial inflammatory responses affect Parkinson's disease (PD) associated nigrostriatal degeneration. This is triggered, in measure, by misfolded, nitrated alpha-synuclein (N-α-syn) contained within Lewy bodies that are released from dying or dead dopaminergic neurons into the extravascular space. N-α-syn-stimulated microglial immunity is regulated by CD4+ T cells. Indeed, CD4+CD25+regulatory T cells (Treg) induce neuroprotective immune responses. This is seen in rodent models of stroke, amyotrophic lateral sclerosis, human immunodeficiency virus associated dementia, and PD. To elucidate the mechanism for Treg-mediated microglial responses, we used a proteomic platform integrating difference gel electrophoresis and tandem mass spectrometry peptide sequencing. These tests served to determine the consequences of Treg on the N-α-syn stimulated microglia. The data demonstrated that Treg substantially alter the microglial proteome in response to N-α-syn. This is seen through Treg's abilities to suppress microglial neurotoxic proteins linked to cell metabolism, migration, protein transport and degradation, redox biology, cytoskeletal, and bioenergetic activities. We conclude that Treg modulate the N-α-syn microglial proteome and, in this way, can slow the tempo and course of PD.

Keywords

Regulatory T cells; Proteomics; Microglia; Inflammation; Parkinson's disease; Alpha-synuclein

Introduction

Parkinson's disease (PD) is a progressive neurodegenerative disease characterized clinically as gait and motor disturbances such as rigidity, resting tremor, slowness of voluntary movement, and postural instability. In some cases these evolve to frank dementia[1-4]. A plethora of host and environmental factors affect the onset and progression of PD including genetics, environmental cues, aging, peripheral immunity, impaired energy metabolism, and oxidative stress[5-15]. Pathologically, PD is characterized by nigrostriatal degeneration precipitated by

*Correspondence and reprint requests to: Howard E. Gendelman, MD, Department of Pharmacology and Experimental Neuroscience, University of Nebraska Medical Center, 985880 Nebraska Medical Center, Omaha, Nebraska 68198-5880, TEL: 402-559-8920, FAX: 402-559-3744, hegendel@unmc.edu.

Supplementary Information. An extended material and methods is available in the supplementary information. This information is available free of charge via the Internet at http://pubs.acs.org.

progressive loss of dopaminergic neuronal cell bodies in the substantia nigra pars compacta (SNpc) and their projections to the dorsal striatum[16]. This degeneration is associated with alterations in innate, microglial activation[17-24] and adaptive T cell immunity[5,25-27]. Precipitation of immune dysfunction in PD is thought to ensue from the release of cytoplasmic inclusions of fibrillar, misfolded proteins encased in Lewy bodies (LB) and composed principally of aggregated α-synuclein (α-syn)[28]. Such misfolded proteins can engage innate and adaptive immunity[28,29]. Indeed, substantive evidence supports the notion that nigrostriatal degeneration is manifest by α-syn mediated microglial activation, oxidative stress and disease inciting adaptive immune responses[25-27, 30-33]. It is the pathogenic spiral of dopaminergic neuronal death, release of extracellular aggregated α-syn, microglial activation, peripheral immune activation, collateral neuronal injury, sustained α-syn release with ingress into lymphatics, and engagement of specific T cell responses that further damage dopamine neurons.

We previously demonstrated that microglia associated degenerative responses are triggered by nitrated α-syn (N-α-syn)-specific effector T cells (Teff)[25]; whereas, CD4+CD25+ regulatory T cells (Treg) attenuate microglial activation and promote dopaminergic neuronal survival[34]. Lacking from our prior works was a mechanism for CD4+ T cell-mediated modulation of microglial function. Based on these observations, we hypothesized that CD4+ T cells have dual roles, and as such, influence microglial responses to evoke biological activities that ultimately effect neuronal survival or loss. In attempts to decipher the mechanisms underlying such responses, we used aggregated N-α-syn as an inducer of microglial activation[30-32], then examined the microglial proteome affected by interactions with CD4+ T cell subsets[35]. Using proteomic approaches, we demonstrate that Treg regulatory activities extend beyond inhibition of cellular activation and include modulation of a broad range of microglial activities involving regulation of phagocytosis and proteasome function, induction of redox-active and bioenergetic proteins, and apoptotic cell processes. Such regulatory events lead to the attenuation of microglial inflammatory neurotoxic responses. Importantly, the data demonstrate that the effects of Treg on N-α-syn-mediated immune activities are multifaceted and of potential therapeutic benefit.

Materials and Methods

Animals

C57BL/6J male mice (7 wks old) were purchased from The Jackson Laboratory (Bar Harbor, ME) and used for CD4+ T cell isolations. C57BL/6J neonates were obtained from breeder colonies housed in the University of Nebraska Medical Center animal facilities. All animal procedures were in accordance with National Institutes of Health guidelines and were approved by the Institutional Animal Care and Use Committee of the University of Nebraska Medical Center.

Cell isolates

Microglia were prepared from neonatal mice (1-2 days old) using previously described techniques[36]. Cultures were consistently >98% CD11b+ microglia[37]. CD4+ T cell subsets were isolated using previously described techniques[34, 38]. Treg and Teff isolates were >95% enriched[35]. CD3-activated T cells were co-cultured with microglia at 1:1 ratio. All analyses of microglia were performed after removal of the T cells from the cultures.

Recombinant α-syn

Purification, nitration and aggregation of recombinant mouse α-syn were performed as previously described[30-32]. N-α-syn was added to cultures at 100 nmol/L (14.5 ng/ml).

2D Difference Gel Electrophoresis (DIGE) and image analysis

Protein prepared from microglial cell lysates was labeled with the respective CyDyes, followed by separation in the first and second dimension, and the gels were scanned using a Typhoon 9400 Variable Mode Imager. Analyses of Cy3-Cy5 image pairs, adjustment to Cy2 control images and detection of protein spots were performed using DeCyder™ software (GE Healthcare). Statistical significance ($P \leq 0.05$) was determined with Biological Variance Analysis (BVA).

Mass spectrometry

In gel trypsin digestion were performed as previously described[40]. The resulting peptides were sequenced using Electrospray Ionization-Liquid Chromatography Mass Spectrometry (ESI-LC MS/MS) (Proteome X System with LCQDecaPlus mass spectrometer, ThermoElectron, Inc.) with a nanospray configuration. The spectra were searched against the NCBI.fasta protein database narrowed to murine proteins using SEQUEST search engine (BioWorks 3.1 SR software from ThermoElectron, Inc.). Validation of select proteins identified by LC-MS/MS was performed using immunocytochemistry or Western blot (Supplementary information)

Cytotoxicity

The Live/Dead Viability/Cytotoxicity kit (Invitrogen) was performed according to manufacturer's protocol. Images were taken using fluorescence microscopy. Cell counts were normalized as the percentage of surviving cells from unstimulated culture controls.

Statistics

For identification of statistically significant proteins, three-to-four analytical gels were analyzed using BVA software by one-way ANOVA for pair-wise comparison between treatment groups. Differences between means ± SEM were analyzed by one-way ANOVA followed by Tukey's post-hoc test for pair-wise comparisons.

Results

Microglial protein profiling techniques following N-α-syn stimulation and Treg co-cultivation

We previously demonstrated that aggregated N-α-syn induces activation of the NF-κB pathway in microglia resulting in a robust inflammatory response characterized by increased production of TNF-α, IFN-γ, IL-6, and IL-1β among others [30, 31]. Co-culture of microglia with Treg either pre- or post-stimulation significantly attenuates NF-κB activation as well as inflammatory cytokine and superoxide production in response to N-α-syn, whereas Teff exacerbate these responses [34, 39]. Therefore, to uncover putative mechanisms for CD4+ T cell-mediated modulation of the microglial phenotype, 2D DIGE was used to identify differences in protein expression of N-α-syn stimulated of microglia alone and co-cultured with CD4+ T cells. 2D DIGE analysis of microglial cell lysates was repeated three separate times with three independent cell isolations and cultures. Analyses of 2D images from protein lysates of 15×10^6 microglial cells identified an average of approximately 2000 “putative” protein spots. DeCyder™ DIGE Analysis of Cy3-labeled proteins from unstimulated microglia and Cy5-labeled proteins from N-α-syn stimulated microglia obtained from three independent experiments showed an average of 2072 detected spots. Representative analyses revealed 43% differentially expressed protein spots after setting a threshold mode of quantitative differences ≥ 2 standard deviations (SD). Of those uniquely identifiable spots (582), 28% were upregulated and (318) 15% were downregulated in microglial cell lysates in response to 24 h stimulation with N-α-syn. To assess how CD4+ T cells modulate the N-α-syn microglial phenotype, microglia were co-cultured with either Treg or Teff for 24 h either prior to stimulation with N-α-syn (pre-treatment) or following 12 h of stimulation (post-treatment), and comparisons were

made using 2D DIGE and *nano*-LC-MS/MS peptide sequencing (Figure 1). Co-cultivation with Treg prior to stimulation with N-α-syn (pre-treatment) altered the microglial phenotypic response to N-α-syn stimulation. An analysis of Cy3-labeled proteins from N-α-syn stimulated microglia and Cy5-labeled proteins from N-α-syn stimulated microglia pre-treated with Treg obtained from three independent experiments showed an average of 2326 detected spots. Representative analysis revealed 31% differentially expressed protein spots after setting a threshold mode of quantitative differences ≥ 2 SD. Of those uniquely identifiable spots (348), 15% were increased and (365) 16% were decreased in microglial cell lysates in response to Treg treatment prior to N-α-syn stimulation. Pre-treatment with Teff had less robust affects on the microglial phenotype in response to N-α-syn. Of the > 2000 uniquely identifiable spots, approximately 32 (1.8%) were decreased and 22 (1.3%) increased in abundance compared to N-α-syn stimulation alone.

To mimic what may occur during overt disease, CD4+ T cells were added to N-α-syn microglial cultures 12 h post-stimulation. Co-cultivation with Treg post-stimulation with N-α-syn (post-treatment) also altered the microglial phenotype. An analysis of Cy3-labeled proteins from N-α-syn stimulated microglia and Cy5-labled proteins from N-α-syn stimulated microglia post-treated with Treg obtained from three independent experiments showed an average of 1905 detected spots. Representative analysis revealed 27% differentially expressed protein spots after setting a threshold mode of quantitative differences ≥ 2 SD. Of those uniquely identifiable spots, (110) 6% were increased and (403) 21% were decreased in microglial cell lysates in response to Treg treatment following N-α-syn stimulation. By comparison, post-treatment with Teff resulted in significant modulation of the microglial proteome in response to N-α-syn stimulation. Of the > 2000 uniquely identifiable spots, approximately 318 (15%) were decreased and 325 (16%) were increased in abundance compared to N-α-syn stimulation alone.

To identify differentially expressed proteins ($P \leq 0.05$), analyses with BVA software were performed on analytical gels from separate lysates comparing microglia cultures stimulated with media alone, N-α-syn or co-cultured with Treg or Teff to facilitate cross-comparisons between treatments by BVA whereby identified spots were compared for area and peak height (3D plots). The 3D peak of each protein spot, comprised of Cy3-labeled and Cy5-labeled cell lysates, was generated based on the pixel intensity versus pixel area, where peak area correlated with the distribution of the protein spot on the gel. 3D images were obtained using 2D Master Imager and were evaluated independently based on their differential fluorescent signal within a constant area for the spot. Their relative peak volumes were normalized to the total volume of the spot (Cy2-labeled). All analytical gels were cross-compared by BVA and matched to a preparative gel consisting of pooled protein from the experimental groups. The proteins identified consisted of structural or cytoskeletal proteins, regulatory proteins, redox-active proteins and enzymes. Figure 2 shows the location of these proteins on the preparative gel selected for LC-MS/MS sequencing.

N-α-syn stimulation and the microglial proteome

In our prior works, we demonstrated that N-α-syn is capable of inducing the temporal activation of a neurotoxic microglial phenotype [30, 31]. To extend these works, the time course of activation was extended from 2 h, 4 h, and 8 h to 24 h for the current study. Table 1 shows proteins differentially expressed in microglia that were stimulated in media alone or with N-α-syn. Proteins were considered identified with high confidence with at least two peptides sequenced and met the threshold peptide criteria (Supplementary information). Such threshold criteria have been determined previously to result in a 95% confidence level in peptide identification[41, 42]. The categories of proteins included regulatory, cytoskeleton/structural, enzymes, mitochondrial, redox-active and others. Figure 3A shows the relative percentages of

proteins within each classification based on protein function that were modulated by N-α-syn stimulation and expression trends.

A majority of the proteins positively identified by mass spectrometry were decreased in expression. A large percentage of the proteins that were decreased in response to N-α-syn stimulation following 24 h were cytoskeletal associated including vimentin, cofilin 1, beta-actin and alpha-tubulin (Table 1). N-α-syn stimulation also resulted in decreased expression of proteins involved in protein processing, transport, and folding. These included cryptochrome 2, 14-3-3 zeta, and annexin A1, as well as several molecular chaperones including heat shock protein (Hsp) 10, Hsp 60, and Hsp 70. Moreover, stimulation with N-α-syn decreased expression of proteins associated with the ubiquitin-proteasome system (UPS) greater than 1.5-fold compared to unstimulated microglia (Table 1). Several proteins associated with mitochondrial function and redox biology were also decreased as a result of stimulation with N-α-syn. Of interest, proteins of the electron transport chain (ETC), specifically complex V involved in adenosine triphosphate (ATP) synthesis, were decreased in expression. Redox-active proteins were also decreased following 24 h of exposure to N-α-syn including superoxide dismutase (Sod)1, biliverdin reductase B, peroxiredoxin (Prdx) 1 and glutaredoxin 1 (Table 1). Other proteins decreased following stimulation with N-α-syn stimulation were metabolic proteins such as acetyl-coenzyme A and aldehyde dehydrogenase, and proteins involved in glycolysis such as alpha enolase, pyruvate dehydrogenase, and pyruvate kinase (Table 1). Despite the even-distribution of up- and down-regulated proteins identified in the initial analysis, many of the proteins that were increased in expression did not reach the confidence interval threshold for adequate identification by mass spectrometry. Nonetheless, those identified included lysosomal proteases cathepsins B and D, gelsolin implicated in inflammation and proteins involved in catabolism including aldo-keto reductase family 1 member B8 and catechol o-methyltransferase (Table 1).

Treg-microglial co-cultivation followed by N-α-syn stimulation (pre-treatment)

To simulate preclinical disease and assess putative mechanisms for early affects of CD4+ T cells on the microglial phenotype in response to N-α-syn, microglial cells were co-cultured with CD3-activated CD4+ T cells for 24 h prior to exposure to N-α-syn. Table 2 shows those proteins differentially expressed in microglia stimulated with N-α-syn alone or pre-treated with Treg. The relative percentages of proteins within each classification based on protein function that were modulated by Treg pre-treatment together with N-α-syn stimulation and expression trends are shown in Figure 3B. Among the proteomic changes induced by pre-treatment of microglia with Treg prior to N-α-syn stimulation were decreased expression in several cytoskeletal proteins such as β-actin, vimentin, cofilin 1, and gelsolin, involved in regulation of cell motility and vesicle transport. Treatment with Treg also resulted in increased expression of microglial proteins involved in exocytosis such as annexin A1 and annexin A4, and phagocytosis such as L-plastin (Table 2). In addition, pre-treatment with Treg increased expression of UPS-related proteins including proteasome subunit alpha type-2, proteasome subunit beta type-2, ubiquitin specific protease 19 and ubiquitin fusion degradation. Treatment with Treg also increased the expression of molecular chaperones including HSPs and calreticulin. Whereas lysosomal proteases cathepsins B and D were increased by N-α-syn stimulation alone, microglia pre-treated with Treg showed decreased abundance of the same proteins. Regulatory proteins involved in cellular metabolism (transaldolase 1) and catabolism (α-mannosidase) were increased in Treg pre-treated cultures (Table 2).

ETC proteins such as nicotinamide adenine dinucleotide (NADH) dehydrogenase (ubiquinone) Fe-S protein-2 of complex I, cytochrome c oxidase of complex III and the subunits that comprise the components of ATP synthase were increased by microglia in response to N-α-syn stimulation following Treg pre-treatment. Changes in the mitochondrial response to Treg

were not limited to proteins involved in cellular energetic, but included redox proteins, chaperones, and structural proteins. Other proteins increased as a result of pre-treatment with Treg were mitochondrial redox-active proteins including peroxiredoxins, Sod 1, Sod 2, thioredoxin (Thrx) 1 and catalase. In addition, cytoplasmic redox-active proteins were also increased including Prdx 1, biliverdin reductase B and glutaredoxin 1 (Table 2).

Cross-comparison of Teff pre-treatments was facilitated by the BVA module to compare protein expression trends. In contrast to pre-treatment with Treg, pre-treatment with Teff did not alter the expression of structural proteins including cofilin 1 and 2, taxilin alpha or beta actin in response to N-α-syn stimulation. Expression of lysomal proteases including cathepsin B and D were also not changed. In addition, pre-treatment with Teff did not affect expression of redox-active proteins such as Prdx 5, cytochrome c reductase, Thrx 1, or biliverdin reductase B. However, enzymatic proteins that were involved in glycolysis and metabolism were decreased in expression following Teff pre-treatment included pyruvate kinase M, phosphoglycerate kinase and aldolase A. Proteins of the ETC were also decreased including ATP synthase (Complex V). Compared to N-α-syn stimulation alone, Teff pre-treatment resulted in greater than 1.5 fold increased expression of voltage-dependent anion channel-1 (Vdac-1), the interferon α/β receptor, and Prdx 1, whereas Hsp 90, chaperonin, galectin 3 and gelsolin were decreased greater than 1.5 fold in expression (data not shown).

N-α-syn stimulation followed by Treg-microglial co-cultivation (post-treatment)

For comparison of the microglial phenotype after commitment to activation by N-α-syn stimulation and modulation by CD3-activated CD4+ T cells, microglia were first stimulated with N-α-syn for 12 h prior to the addition of Treg or Teff for an additional 24 h and the T cells removed prior to microglial cell lysis. Table 3 shows those proteins differentially expressed in microglia stimulated with N-α-syn alone or post-treated with Treg. The relative percentages of proteins within each classification based on protein function that were modulated by Treg post-treatment together with N-α-syn stimulation and expression trends is shown in Figure 3C.

Similar proteins were affected by post-treatment with Treg as with pre-treatment; interestingly, some exhibited opposite expression patterns observed after pre-treatment with Treg. Akin to pre-treatment, post-treatment with Treg yielded increased redox-active protein expression by activated microglia including Sod1 and Prdx1 and 5. Several proteins differentially expressed in the pre-treatment analysis were also identified in post-treatment analysis, but were expressed in opposite directions, including increased expression of structural proteins involved in cell motility, such as β-actin and γ-actin, decreased expression of mitochondrial proteins including ETC complex V, and decreased expression of L-plastin (Table 3). Induction of pro-apoptotic protein expression was observed and included increased expression of apoptosis-associated speck-like protein containing a caspase recruitment domain, gelsolin, eukaryotic translation elongation factor 1, and cathepsins B and D. Decreased expression of proteins involved in cellular metabolism such as aldolase I and aldehyde dehydrogenase 2 was also observed in response to Treg post-treatment (Table 3).

Cross-comparison of protein expression trends following post-treatment with Teff revealed that in contrast to pre-treatment, post-treatment with Teff increased expression of redox-active proteins including Prdx 1, Thrx 1, and cytochrome c oxidase in N-α-syn stimulated microglia compared to N-α-syn stimulation alone. Ferritin light chain, Hsp 70, and transaldolase 1 were also increased. Similar to pre-treatment, expression of cathepsins B and D were not affected. Moreover, expression of pro-apoptotic proteins was not affected with Teff post-treatment (data not shown).

Validation of protein identification and biological significance

Immunocytochemistry and Western blot analyses were used to validate protein expression trends identified in our proteomic analyses. Immunoflourescent cytochemistry revealed that stimulation with N-α-syn significantly reduced Prx1 expression in microglial cells compared to unstimulated microglia. In contrast, Treg pre-treatment protected against a decrease in Prx1 expression (Fig. 4A). In comparison, post-treatment with Treg rescued microglial Prx1 expression and restored expression levels to near 100% of the unstimulated control. The effect of Teff was more variable and depended on the temporal engagement of Teff with stimulated microglia. Pre-treatment with Teff did not effectively alter Prx1 expression in response to N-α-syn stimulation, however Prx1 expression appeared to be partially rescued following post-treatment with Teff although this did not reach statistical significance.

Western blot validation for cytoskeletal and inflammatory proteins that were involved both in cell mobilization as well as survival, confirmed expression trends of select proteins following different culture conditions (Fig. 4B). Expression of alpha-tubulin was decreased nearly 6-fold following Treg pre-treatment, and compared to a 1.5 fold increase by N-α-syn stimulation alone. In comparison, alpha tubulin expression in N-α-syn–stimulated microglia following Teff pre-treatment was reduced by 2-fold. Post-treatment with Treg or Teff failed to alter alpha-tubulin expression levels in N-α-syn stimulated microglia. Analysis of gelsolin confirmed the increased expression in N-α-syn stimulated microglial lysates compared to control (1.5 fold). Pre-treatment with Treg reduced gelsolin expression to control levels, while, post-treatment increased gelsolin expression compared to N-α-syn stimulation alone. Albeit pre-treatment with Treg had no effect on galectin 3 expression, post-treatment with Treg resulted in a 1.4 fold increase compared to N-α-syn stimulation alone. No change in expression of gelsolin or galectin 3 was detected in response to Teff treatment by Western blot.

Immunofluorescence cytochemistry for actin and Hsp70 also confirmed differential expression of these proteins following N-α-syn stimulation and pre-treatment with CD4+ T cells. Whereas pre-treatment with Treg significantly decreased fluorescence intensity of beta-actin expression in response to N-α-syn stimulation, expression of Hsp70 was increased compared with N-α-syn stimulation alone to levels and exceeded those observed in unstimulated controls. By comparison, pre-treatment with Teff had no observed affect on either actin or Hsp70 expression compared with N-α-syn stimulation alone (Fig 4C).

Deleterious microglial activation is postulated to affect a neurodegenerative process in PD. For this reason, suppression of microglial activation by Treg may be responsible for the profound protection observed *in vivo*[34]. To investigate whether phenotypic modulation of microglia by Treg co-culture affected neuronal survival, an *in vitro* model of microglia-mediated cytotoxicity was established using N-α-syn-activated microglia and the dopaminergic cell line MES23.5. We observed a 56% loss of MES23.5 cells after co-culture for 24 h with N-α-syn stimulated microglia compared to control co-cultures of MES23.5 with unstimulated microglia (Fig. 4D). In contrast, co-culture of N-α-syn stimulated microglia with Treg inhibited microglial-mediated MES23.5 cytotoxicity, while activated Teff afforded no cytotoxic protection. These data suggested that Treg modulation of microglia attenuates the neurocytotoxic responses mediated by activated microglia. In addition, supernatants from microglia stimulated with N-α-syn alone or N-α-syn and cultured in the presence of Teff were cytotoxic to MES23.5 cells, whereas neurocytotoxicity was abrogated in supernatants from stimulated microglia co-cultured with Treg. Surprisingly, there was less cytotoxicity induced from culture supernatants from N-α-syn microglia treated with Teff than seen in supernatants from N-α-syn microglia alone. How this occurred awaits further study. These data demonstrate the potential of Tregs to suppress cytotoxicity afforded by N-α-syn-activated microglia, and suggest that direct modulation of microglial responses provides a primary mechanism for Treg-mediated neuronal protection.

Discussion

The events that lead to microglial activation in PD and its effects on neuronal survival can be attributed to the formation of aggregated α-syn in the cytosol or in LB, the death of dopaminergic neurons, and the release of these modified aggregates to activate microglia and induce a lethal cascade of neuroinflammation and neuronal destruction[33, 43]. Oxidation of α-syn leads to formation of aggregates and filaments found to be a major component of LB[44, 45]. α-Syn released from dying dopaminergic neurons activates microglia, causing release of reactive oxygen species (ROS) and neurotoxicity[30-34]. Indeed, oxidized and aggregated α-syn, when released from dying neurons, may stimulate scavenger receptors on microglia resulting in their sustained activation and dopaminergic neurodegeneration[29, 33, 43]. Alternatively, microglia may internalize α-syn through the formation of clathrin pits and secondarily activate microglia[46]. Activated microglia generate nitric oxide and superoxide that rapidly react to form peroxynitrite[47], which can then traverse cell membranes resulting in nitrotyrosine formation and further nitration of α-syn, DNA damage, mitochondrial inhibition, and lipid peroxidation[48]. The mechanisms by which α-syn activates microglia have been extensively studied and include endocytosis of α-syn by microglia with subsequent cell stimulation resulting in NF-κB activation and secretion of pro-inflammatory cytokines and chemokines as well as production of ROS[30, 33, 46]. Moreover, α-syn alters the microglial genome, proteome, and secretome leading to the temporal conversion from a neuroregulatory phenotype to an activated phenotype; the latter characterized by differential expression of regulatory, structural, and redox-active proteins, and enzymes together with altered biochemical functions including protein processing, trafficking and degradation[30, 31].

Microglia serve as the first line of defense and protects the host against pathogenic microbes through phagocytosis, antigen presentation, and secretion of biologically active factors, as well as mediation of pathological processes. During homeostatic conditions, microglial cells are in a resting state, their cell bodies barely visible and few ramified processes. Neuroprotective functions of homeostatic microglia are suggested by their abilities to produce neurotrophins and eliminate excitotoxins present in the extracellular spaces[49] and may also promote neuronal survival following injury[50, 51]. Underlying these cellular functions is inflammation. Altogether, the inflammatory process serves as a sensor against invasion of bacteria, viruses, and parasites, as well as wound healing following acute tissue infection and injury. However, inflammation is closely linked to neurodegenerative processes. In the central nervous system (CNS), neuroinflammation perpetrated through activation of microglia and other glial elements act in concert as a central pathway in a multitude of neurodegenerative disorders including PD. These initial responders of innate immunity set up a cascade, and later involve the activation and recruitment of adaptive immunity and ultimately neurodegeneration.

A role for adaptive immunity in the pathogenesis of PD has been proposed as a result of several independent lines of investigation that demonstrated a robust adaptive immune response to the CNS consisting of T cell and B cell infiltration, and immunoglobulin deposition within the SNpc to a greater extent than could be attributed to normal immune surveilence[5, 25-27]. Importantly, an intact adaptive immune system with functional CD4+ T cells are required for 1-methyl-4-phenyl-1,2,3,6-tetrahydropyridine (MPTP)-induced Parkinsonism in rodents[26]. As microglial activation is a key pathological feature of PD, we hypothesized that microglial interactions with specific CD4+ T cell subsets may affect the microglial activation phenotype and thus the tempo of disease. Specifically, we posited that interactions with Teff would exacerbate neurotoxic responses whereas Treg would attenuate microglial activation. This is in contrast to current hypotheses that a synergistic immune response between Th1 and Th2 modulate the microglial neurotoxic phenotype to neuroprotective[52, 53]. According to this hypothesis, synergy between IFN-γ and IL-4 is necessary to modulate neuroprotective innate immunity, in that protection cannot be afforded without the innate immune cells first being

activated. However, during neurodegenerative disease, microglia and astrocytes are already in the activated state and induce Th1 responses that exacerbate the microglial neurotoxic phenotype, whereas the induction of Th2/Treg responses would effectively attenuate disease pathogenesis [39, 54].

Genomic and proteomic methodologies are widely used to evaluate changes in gene transcripts and protein expression linked to PD pathogenesis. Analyses of SN of PD patients revealed dysregulation in gene expression, including substantial down-regulation of genes involved in synapse function, dopaminergic phenotype, cytoskeletal maintenance[60],and components of the proteasome and ETC complexes[61]. The results of which provide support for the impairment of multiple ETC complexes and the UPS in PD. Of these, genes involved in the ETC[62], as well as genes encoding components of the UPS were decreased. These analyses also revealed an upregulation of genes that participate in protein disposal and degradation[60], induction of HSPs, anti-apoptotic gene groups, and genes involved in mitogenic pathways[62]. Analysis of protein expression of the SN from PD patients implicates an inflammatory process in disease pathogenesis. Higher expression of redox-active proteins[64], along with reduced complex I, II, and III activity was also identified to support this contention. Studies have thus far revealed relatively comprehensive quantitative changes in gene expression and protein expression, as well as post-translational modifications (mostly oxidative damage) of high abundance proteins, thus confirming deficits in energy production, protein degradation, antioxidant protein function, and cytoskeletal regulation associated with neurodegenerative diseases such as PD[65-72].

Interaction between Treg and microglia affect microglial processes including inflammation, cell function, and specific enzymatic activities ultimately resulting in the conversion of microglia from a neurotoxic to neuroprotective phenotype. This change is multifunctional as the microglial response to stimuli can induce reversion to its original function in maintenance of homeostasis and prevention of neuronal damage. We show that the cellular proteome of microglia in response to N-α-syn stimulation is modulated by pre-treatment with Treg and consists of increased expression of redox-active proteins, altered expression of cytoskeletal proteins involved in phagocytosis and migration, increased expression of HSPs and proteins of the UPS, increased expression of proteins of the ETC, and decreased expression of lysosomal proteases. Taken together, our data suggest that Treg are able to facilitate microglial homeostatic functions to cope with oxidative stress and accumulation of aberrant proteins. Indeed, HSPs have been shown to protect cells from toxicity associated with inhibition of proteasomal function and form excess levels of normal or abnormal proteins[55, 56]. As inhibition of the proteasomal system has been implicated in PD pathogenesis, stimulation of UPS-mediated proteolysis could serve as a potential therapeutic avenue induced by Treg to reduce protein aggregation and pathology linked to PD. As disease progresses, the effects of Treg on the microglial phenotype may be subverted as a result of reduced numbers or function of Treg, reduced microglial susceptibility to Treg regulation or robust effector T cell responses that overwhelm regulatory functions. The result is a compromise of microglial function and homeostasis and induction of an inflammatory phenotype that mediates neurodegenerative processes.

Proteomic changes observed by addition of Treg post-treatment were less robust than with pre-treatment. In keeping with prior studies, the proteomic profile of the stimulated microglia following co-culture with Treg revealed increased expression of apoptotic proteins, which parallel decreased expression in proteins related to ATP synthesis and cellular metabolism. N-α-syn induces ROS production and NF-κB activation by microglia[30-32], and oxidative modification of several proteins may result in altered structure and function or targeted degradation following treatment with Treg that were not targeted with pre-treatment. Less robust changes observed with post-treatment may also be attributed to increased caspase

activation and apoptosis of microglia[35] resulting in altered protein synthesis and processing. Increased expression of lysosomal proteases including cathepsins B and D suggest that post-stimulatory Treg interactions induce autolysis[57]. Indeed, we have shown that the pro-apoptotic effect of Tregs on activated microglia is mediated, in part, by the Fas-FasL pathway and is contingent on cathepsin B expression[35].

A novel hypothesis for Treg modulation of microglial function during the asymptomatic and overt disease stages in PD is proposed. This hypothesis is based on the activation of innate immune responses by aggregated and oxidized neural proteins, particularly α-syn. We posit that during the asymptomatic stage, adaptive immune responses are operative on microglia that attenuate microglial activation and neuroinflammatory responses including ROS that parallel nigral neuronal damage and subsequent release of α-syn from LB. Treg at this stage of disease modulate microglia to be actively phagocytic and produce a spectrum of regulatory factors that maintain CNS homeostasis. This limits accumulation of α-syn in the extravascular space. Such biochemical events preclude the development of potent neurodegenerative immune responses and the widespread, often adverse affects of oxidized and misfolded proteins. During overt disease, regulation of adaptive immunity breaks down and significantly influences control of the neural environment[25, 26]. Indeed, the effects of aging on microglial function have been proposed to result in chronic microgliosis or cellular senescence leading to the production of pro-inflammatory and neurotoxic mediators[58, 59]. Treg may also be, in part, reduced in numbers and function as a result of age, decreased T cell receptor repertoire and N-α-syn immunity. However, clinical analyses of T cell subsets yielded conflicting results in regards to CD4+CD25+ Treg numbers and function[5,11] for aging and PD. Nonetheless, the neuroinflammatory events seen in disease are known to result in more widespread nigrostriatal damage, recruitment of immunocytes into the brain and a spiral of pathogenic activities facilitating accelerated neuronal damage and loss. Profound oxidative-associated neuronal damage and death of nigral neurons lead to increased release of α-syn and drives subsequent oxidation and folding. With increased exposure to N-α-syn, microglia are activated yielding a phenotype with reduced phagocytic capacity and homeostatic secretory processes. During this phase, Treg likely engages activated microglia for apoptosis or affect neurotrophic activities while showing limited, in part, pro-inflammatory activity. Our results, taken together, demonstrate the importance of adaptive immune responses in the tempo, progression and control of PD. How such immunomodulators can be controlled for the benefit of the patient will continue to be a target area for future research.

Conclusion

These studies corroborate observations of others[73-75] that uncover important differences in the mechanism of Treg-mediated suppression of inflammation. While pre-treatment with Treg alter the microglial activation phenotype to stimulation, Treg interactions following stimuli-mediated activation induce apoptosis. The ability of Treg to regulate microglial inflammation, cell function, and specific enzymatic activities provide novel tools to manipulate ongoing microglial inflammatory responses. In light of these and previously published findings, we now propose a model for disease with regards to a role for Treg in both the pathogenesis and therapeutic intervention of PD. As such, these data support the use of therapeutics that manipulates Treg responses within the brain or that target specific protein changes linked to reversion of a neurotoxic microglial phenotype to neurotrophic.

Supplementary Material

Refer to Web version on PubMed Central for supplementary material.

Acknowledgments

The authors thank Drs. Tong Wang, Eric Anderson, Pawel Ciborowski, Joshua Schlautman, Dr. Ronald Cerny for technical assistance and data analysis, and Robin Taylor for critical reading of the manuscript. This work was funded by the Frances and Louie Blumkin Foundation, the Community Neuroscience Pride of Nebraska Research Initiative, the Alan Baer Charitable Trust (to H.E.G.), the UNMC Patterson Fellowship (to A.D.R.), and NIH grants 5P01NS31492, 2R37 NS36126, 2R01 NS034239, P20RR15635, U54NS43011, P01MH64570 and P01 NS43985 (to H.E.G.).

References

1. Dauer W, Przedborski S. Parkinson's disease: mechanisms and models. Neuron 2003;39(6):889–909. [PubMed: 12971891]
2. Fahn, S.; Przedborski, S. Parkinsonism. In: Rowland, LP., editor. Merritt's Neurology. Lippincott Williams & Wilkins; New York: 2000. p. 679-693.
3. Fahn S, Sulzer D. Neurodegeneration and neuroprotection in Parkinson disease. NeuroRx 2004;1(1): 139–54. [PubMed: 15717014]
4. Mayeux R. Epidemiology of neurodegeneration. Annu Rev Neurosci 2003;26:81–104. [PubMed: 12574495]
5. Baba Y, Kuroiwa A, Uitti RJ, Wszolek ZK, Yamada T. Alterations of T-lymphocyte populations in Parkinson disease. Parkinsonism Relat Disord 2005;11(8):493–8. [PubMed: 16154792]
6. Klockgether T. Parkinson's disease: clinical aspects. Cell Tissue Res 2004;318(1):115–20. [PubMed: 15365814]
7. Linton PJ, Dorshkind K. Age-related changes in lymphocyte development and function. Nat Immunol 2004;5(2):133–9. [PubMed: 14749784]
8. Naylor K, Li G, Vallejo AN, Lee WW, Koetz K, Bryl E, Witkowski J, Fulbright J, Weyand CM, Goronzy JJ. The influence of age on T cell generation and TCR diversity. J Immunol 2005;174(11): 7446–52. [PubMed: 15905594]
9. Orr CF, Rowe DB, Mizuno Y, Mori H, Halliday GM. A possible role for humoral immunity in the pathogenesis of Parkinson's disease. Brain 2005;128(Pt 11):2665–74. [PubMed: 16219675]
10. Reale M, Iarlori C, Thomas A, Gambi D, Perfetti B, Di Nicola M, Onofrj M. Peripheral cytokines profile in Parkinson's disease. Brain Behav Immun. 2008
11. Rosenkranz D, Weyer S, Tolosa E, Gaenslen A, Berg D, Leyhe T, Gasser T, Stoltze L. Higher frequency of regulatory T cells in the elderly and increased suppressive activity in neurodegeneration. J Neuroimmunol 2007;188(12):117–27. [PubMed: 17582512]
12. Sian J, Dexter DT, Lees AJ, Daniel S, Agid Y, Javoy-Agid F, Jenner P, Marsden CD. Alterations in glutathione levels in Parkinson's disease and other neurodegenerative disorders affecting basal ganglia. Ann Neurol 1994;36(3):348–55. [PubMed: 8080242]
13. Taki J, Nakajima K, Hwang EH, Matsunari I, Komai K, Yoshita M, Sakajiri K, Tonami N. Peripheral sympathetic dysfunction in patients with Parkinson's disease without autonomic failure is heart selective and disease specific. Eur J Nucl Med 2000;27(5):566–73. [PubMed: 10853813]
14. Tanner CM. Occupational and environmental causes of parkinsonism. Occup Med 1992;7(3):503–13. [PubMed: 1496432]
15. Tanner CM. Epidemiology of Parkinson's disease. Neurol Clin 1992;10(2):317–29. [PubMed: 1584176]
16. Hornykiewicz O, Kish SJ. Biochemical pathophysiology of Parkinson's disease. Adv Neurol 1987;45:19–34. [PubMed: 2881444]
17. Banati RB, Daniel SE, Blunt SB. Glial pathology but absence of apoptotic nigral neurons in long-standing Parkinson's disease. Mov Disord 1998;13(2):221–7. [PubMed: 9539333]
18. Block ML, Wu X, Pei Z, Li G, Wang T, Qin L, Wilson B, Yang J, Hong JS, Veronesi B. Nanometer size diesel exhaust particles are selectively toxic to dopaminergic neurons: the role of microglia, phagocytosis, and NADPH oxidase. Faseb J 2004;18(13):1618–20. [PubMed: 15319363]
19. Cicchetti F, Brownell AL, Williams K, Chen YI, Livni E, Isacson O. Neuroinflammation of the nigrostriatal pathway during progressive 6-OHDA dopamine degeneration in rats monitored by immunohistochemistry and PET imaging. Eur J Neurosci 2002;15(6):991–8. [PubMed: 11918659]

20. Forno LS, DeLanney LE, Irwin I, Di Monte D, Langston JW. Astrocytes and Parkinson's disease. Prog Brain Res 1992;94:429–436. [PubMed: 1287728]
21. Hong JS. Role of inflammation in the pathogenesis of Parkinson's disease: models, mechanisms, and therapeutic interventions. Ann N Y Acad Sci 2005;1053:151–2. [PubMed: 16179518]
22. McGeer PL, McGeer EG. Glial cell reactions in neurodegenerative diseases: pathophysiology and therapeutic interventions. Alzheimer Dis Assoc Disord 1998;12:S1–6. [PubMed: 9769023]
23. Mirza B, Hadberg H, Thomsen P, Moos T. The absence of reactive astrocytosis is indicative of a unique inflammatory process in Parkinson's disease. Neuroscience 2000;95:425–432. [PubMed: 10658622]
24. Wang X, Chen S, Ma G, Ye M, Lu G. Involvement of proinflammatory factors, apoptosis, caspase-3 activation and Ca2+ disturbance in microglia activation-mediated dopaminergic cell degeneration. Mech Ageing Dev 2005;126(12):1241–54. [PubMed: 16112714]
25. Benner EJ, Banerjee R, Reynolds AD, Sherman S, Pisarev VM, Tsiperson V, Nemachek C, Ciborowski P, Przedborski S, Mosley RL, Gendelman HE. Nitrated alpha-synuclein immunity accelerates degeneration of nigral dopaminergic neurons. PLoS ONE 2008;3(1):e1376. [PubMed: 18167537]
26. Brochard V, Combadiere B, Prigent A, Laouar Y, Perrin A, Beray-Berthat V, Bonduelle O, Alvarez-Fischer D, Callebert J, Launay JM, Duyckaerts C, Flavell RA, Hirsch EC, Hunot S. Infiltration of CD4+ lymphocytes into the brain contributes to neurodegeneration in a mouse model of Parkinson disease. J Clin Invest 2009;119(1):182–92. [PubMed: 19104149]
27. Theodore S, Cao S, McLean PJ, Standaert DG. Targeted overexpression of human alpha-synuclein triggers microglial activation and an adaptive immune response in a mouse model of Parkinson disease. J Neuropathol Exp Neurol 2008;67(12):1149–58. [PubMed: 19018246]
28. Spillantini MG, Schmidt ML, Lee VM, Trojanowski JQ, Jakes R, Goedert M. Alpha-synuclein in Lewy bodies. Nature 1997;388(6645):839–40. [PubMed: 9278044]
29. Croisier E, Moran LB, Dexter DT, Pearce RK, Graeber MB. Microglial inflammation in the parkinsonian substantia nigra: relationship to alpha-synuclein deposition. J Neuroinflammation 2005;2:14. [PubMed: 15935098]
30. Reynolds AD, Glanzer JG, Kadiu I, Ricardo-Dukelow M, Chaudhuri A, Ciborowski P, Cerny R, Gelman B, Thomas MP, Mosley RL, Gendelman HE. Nitrated alpha-synuclein-activated microglial profiling for Parkinson's disease. J Neurochem 2008;104(6):1504–25. [PubMed: 18036154]
31. Reynolds AD, Kadiu I, Garg SK, Glanzer JG, Nordgren T, Ciborowski P, Banerjee R, Gendelman HE. Nitrated alpha-synuclein and microglial neuroregulatory activities. J Neuroimmune Pharmacol 2008;3(2):59–74. [PubMed: 18202920]
32. Thomas MP, Chartrand K, Reynolds A, Vitvitsky V, Banerjee R, Gendelman HE. Ion channel blockade attenuates aggregated alpha synuclein induction of microglial reactive oxygen species: relevance for the pathogenesis of Parkinson's disease. J Neurochem 2007;100(2):503–19. [PubMed: 17241161]
33. Zhang W, Wang T, Pei Z, Miller DS, Wu X, Block ML, Wilson B, Zhou Y, Hong JS, Zhang J. Aggregated alpha-synuclein activates microglia: a process leading to disease progression in Parkinson's disease. Faseb J 2005;19(6):533–42. [PubMed: 15791003]
34. Reynolds AD, Banerjee R, Liu J, Gendelman HE, Mosley RL. Neuroprotective activities of CD4 +CD25+ regulatory T cells in an animal model of Parkinson's disease. J Leukoc Biol 2007;82(5): 1083–94. [PubMed: 17675560]
35. Reynolds AD, Stone DK, Mosley RL, Gendelman HE. Nitrated alpha-synuclein induced alteration in microglial immunity is regulated by CD4+ T cell subsets. J Immunol 2009;182(7):4137–49. [PubMed: 19299711]
36. Dobrenis K. Microglia in cell culture and in transplantation therapy for central nervous system disease. Methods 1998;16(3):320–44. [PubMed: 10071070]
37. Enose Y, Destache CJ, Mack AL, Anderson JR, Ullrich F, Ciborowski PS, Gendelman HE. Proteomic fingerprints distinguish microglia, bone marrow, and spleen macrophage populations. Glia 2005;51 (3):161–72. [PubMed: 15795904]

38. Banerjee R, Mosley RL, Reynolds AD, Dhar A, Jackson-Lewis V, Gordon PH, Przedborski S, Gendelman HE. Adaptive immune neuroprotection in G93A-SOD1 amyotrophic lateral sclerosis mice. PLoS ONE 2008;3(7):e2740. [PubMed: 18648532]
39. Reynolds AD, Stone DK, Mosley RL, Gendelman HE. Nitrated {alpha}-synuclein-induced alterations in microglial immunity are regulated by CD4+ T cell subsets. J Immunol 2009;182(7):4137–49. [PubMed: 19299711]
40. Ciborowski P, Enose Y, Mack A, Fladseth M, Gendelman HE. Diminished matrix metalloproteinase 9 secretion in human immunodeficiency virus-infected mononuclear phagocytes: modulation of innate immunity and implications for neurological disease. J Neuroimmunol 2004;157(12):11–6. [PubMed: 15579275]
41. Ciborowski P, Kadiu I, Rozek W, Smith L, Bernhardt K, Fladseth M, Ricardo-Dukelow M, Gendelman HE. Investigating the human immunodeficiency virus type 1-infected monocyte-derived macrophage secretome. Virology 2007;363(1):198–209. [PubMed: 17320137]
42. Ricardo-Dukelow M, Kadiu I, Rozek W, Schlautman J, Persidsky Y, Ciborowski P, Kanmogne GD, Gendelman HE. HIV-1 infected monocyte-derived macrophages affect the human brain microvascular endothelial cell proteome: new insights into blood-brain barrier dysfunction for HIV-1-associated dementia. J Neuroimmunol 2007;185(12):37–46. [PubMed: 17321604]
43. Wersinger C, Sidhu A. An inflammatory pathomechanism for Parkinson's disease? Curr Med Chem 2006;13(5):591–602. [PubMed: 16515523]
44. Giasson BI, Duda JE, Murray IV, Chen Q, Souza JM, Hurtig HI, Ischiropoulos H, Trojanowski JQ, Lee VM. Oxidative damage linked to neurodegeneration by selective alpha-synuclein nitration in synucleinopathy lesions. Science 2000;290(5493):985–9. [PubMed: 11062131]
45. Souza JM, Giasson BI, Chen Q, Lee VM, Ischiropoulos H. Dityrosine cross-linking promotes formation of stable alpha -synuclein polymers. Implication of nitrative and oxidative stress in the pathogenesis of neurodegenerative synucleinopathies. J Biol Chem 2000;275(24):18344–9. [PubMed: 10747881]
46. Liu J, Zhou Y, Wang Y, Fong H, Murray TM, Zhang J. Identification of proteins involved in microglial endocytosis of alpha-synuclein. J Proteome Res 2007;6(9):3614–27. [PubMed: 17676786]
47. Dringen R. Oxidative and antioxidative potential of brain microglial cells. Antioxid Redox Signal 2005;7(910):1223–33. [PubMed: 16115027]
48. Ischiropoulos H. Oxidative modifications of alpha-synuclein. Ann N Y Acad Sci 2003;991:93–100. [PubMed: 12846977]
49. Schwartz M. Macrophages and microglia in central nervous system injury: are they helpful or harmful? J Cereb Blood Flow Metab 2003;23(4):385–94. [PubMed: 12679714]
50. Batchelor PE, Liberatore GT, Wong JY, Porritt MJ, Frerichs F, Donnan GA, Howells DW. Activated macrophages and microglia induce dopaminergic sprouting in the injured striatum and express brain-derived neurotrophic factor and glial cell line-derived neurotrophic factor. J Neurosci 1999;19(5): 1708–16. [PubMed: 10024357]
51. Batchelor PE, Porritt MJ, Martinello P, Parish CL, Liberatore GT, Donnan GA, Howells DW. Macrophages and Microglia Produce Local Trophic Gradients That Stimulate Axonal Sprouting Toward but Not beyond the Wound Edge. Mol Cell Neurosci 2002;21(3):436–53. [PubMed: 12498785]
52. Garg SK, Kipnis J, Banerjee R. IFN-gamma and IL-4 differentially shape metabolic responses and neuroprotective phenotype of astrocytes. J Neurochem 2009;108(5):1155–66. [PubMed: 19141080]
53. Butovsky O, Talpalar AE, Ben-Yaakov K, Schwartz M. Activation of microglia by aggregated beta-amyloid or lipopolysaccharide impairs MHC-II expression and renders them cytotoxic whereas IFN-gamma and IL-4 render them protective. Mol Cell Neurosci 2005;29(3):381–93. [PubMed: 15890528]
54. Yamamoto M, Kiyota T, Walsh SM, Liu J, Kipnis J, Ikezu T. Cytokine-mediated inhibition of fibrillar amyloid-beta peptide degradation by human mononuclear phagocytes. J Immunol 2008;181(6): 3877–86. [PubMed: 18768842]
55. Fan GH, Zhou HY, Yang H, Chen SD. Heat shock proteins reduce alpha-synuclein aggregation induced by MPP+ in SK-N-SH cells. FEBS Lett 2006;580(13):3091–8. [PubMed: 16678164]

56. Uryu K, Richter-Landsberg C, Welch W, Sun E, Goldbaum O, Norris EH, Pham CT, Yazawa I, Hilburger K, Micsenyi M, Giasson BI, Bonini NM, Lee VM, Trojanowski JQ. Convergence of heat shock protein 90 with ubiquitin in filamentous alpha-synuclein inclusions of alpha-synucleinopathies. Am J Pathol 2006;168(3):947–61. [PubMed: 16507910]
57. Bird PI. Regulation of pro-apoptotic leucocyte granule serine proteinases by intracellular serpins. Immunol Cell Biol 1999;77(1):47–57. [PubMed: 10101686]
58. Choi DY, Zhang J, Bing G. Aging enhances the neuroinflammatory response and alpha-synuclein nitration in rats. Neurobiol Aging. 2008in press
59. Miller KR, Streit WJ. The effects of aging, injury and disease on microglial function: a case for cellular senescence. Neuron Glia Biol 2007;3(3):245–53. [PubMed: 18634615]
60. Wang YM, Pu P, Le WD. ATP depletion is the major cause of MPP+ induced dopamine neuronal death and worm lethality in alpha-synuclein transgenic C. elegans. Neurosci Bull 2007;23(6):329–35. [PubMed: 18064062]
61. Stack EC, Ferro JL, Kim J, Del Signore SJ, Goodrich S, Matson S, Hunt BB, Cormier K, Smith K, Matson WR, Ryu H, Ferrante RJ. Therapeutic attenuation of mitochondrial dysfunction and oxidative stress in neurotoxin models of Parkinson's disease. Biochim Biophys Acta 2008;1782(3):151–62. [PubMed: 18206128]
62. Cole NB, Dieuliis D, Leo P, Mitchell DC, Nussbaum RL. Mitochondrial translocation of alpha-synuclein is promoted by intracellular acidification. Exp Cell Res 2008;314(10):2076–2089. [PubMed: 18440504]
63. Gan L, Ye S, Chu A, Anton K, Yi S, Vincent VA, von Schack D, Chin D, Murray J, Lohr S, Patthy L, Gonzalez-Zulueta M, Nikolich K, Urfer R. Identification of cathepsin B as a mediator of neuronal death induced by Abeta-activated microglial cells using a functional genomics approach. J Biol Chem 2004;279(7):5565–72. [PubMed: 14612454]
64. Reinheckel T, Deussing J, Roth W, Peters C. Towards specific functions of lysosomal cysteine peptidases: phenotypes of mice deficient for cathepsin B or cathepsin L. Biol Chem 2001;382(5): 735–41. [PubMed: 11517926]
65. Abdi F, Quinn JF, Jankovic J, McIntosh M, Leverenz JB, Peskind E, Nixon R, Nutt J, Chung K, Zabetian C, Samii A, Lin M, Hattan S, Pan C, Wang Y, Jin J, Zhu D, Li GJ, Liu Y, Waichunas D, Montine TJ, Zhang J. Detection of biomarkers with a multiplex quantitative proteomic platform in cerebrospinal fluid of patients with neurodegenerative disorders. J Alzheimers Dis 2006;9(3):293–348. [PubMed: 16914840]
66. Basso M, Giraudo S, Corpillo D, Bergamasco B, Lopiano L, Fasano M. Proteome analysis of human substantia nigra in Parkinson's disease. Proteomics 2004;4(12):3943–52. [PubMed: 15526345]
67. Chin MH, Qian WJ, Wang H, Petyuk VA, Bloom JS, Sforza DM, Lacan G, Liu D, Khan AH, Cantor RM, Bigelow DJ, Melega WP, Camp DG 2nd, Smith RD, Smith DJ. Mitochondrial dysfunction, oxidative stress, and apoptosis revealed by proteomic and transcriptomic analyses of the striata in two mouse models of Parkinson's disease. J Proteome Res 2008;7(2):666–77. [PubMed: 18173235]
68. Jin J, Li GJ, Davis J, Zhu D, Wang Y, Pan C, Zhang J. Identification of novel proteins associated with both alpha-synuclein and DJ-1. Mol Cell Proteomics 2007;6(5):845–59. [PubMed: 16854843]
69. Jin J, Meredith GE, Chen L, Zhou Y, Xu J, Shie FS, Lockhart P, Zhang J. Quantitative proteomic analysis of mitochondrial proteins: relevance to Lewy body formation and Parkinson's disease. Brain Res Mol Brain Res 2005;134(1):119–38. [PubMed: 15790536]
70. McLaughlin P, Zhou Y, Ma T, Liu J, Zhang W, Hong JS, Kovacs M, Zhang J. Proteomic analysis of microglial contribution to mouse strain-dependent dopaminergic neurotoxicity. Glia 2006;53(6): 567–82. [PubMed: 16419087]
71. Zhang Y, James M, Middleton FA, Davis RL. Transcriptional analysis of multiple brain regions in Parkinson's disease supports the involvement of specific protein processing, energy metabolism, and signaling pathways, and suggests novel disease mechanisms. Am J Med Genet B Neuropsychiatr Genet 2005;137(1):5–16. [PubMed: 15965975]
72. Zhou Y, Wang Y, Kovacs M, Jin J, Zhang J. Microglial activation induced by neurodegeneration: a proteomic analysis. Mol Cell Proteomics 2005;4(10):1471–9. [PubMed: 15975914]

73. Taams LS, van Amelsfort JM, Tiemessen MM, Jacobs KM, de Jong EC, Akbar AN, Bijlsma JW, Lafeber FP. Modulation of monocyte/macrophage function by human CD4+CD25+ regulatory T cells. Hum Immunol 2005;66(3):222–30. [PubMed: 15784460]

74. Tiemessen MM, Jagger AL, Evans HG, van Herwijnen MJ, John S, Taams LS. CD4+CD25+Foxp3+ regulatory T cells induce alternative activation of human monocytes/macrophages. Proc Natl Acad Sci U S A 2007;104(49):19446–51. [PubMed: 18042719]

75. Venet F, Pachot A, Debard AL, Bohe J, Bienvenu J, Lepape A, Powell WS, Monneret G. Human CD4+CD25+ regulatory T lymphocytes inhibit lipopolysaccharide-induced monocyte survival through a Fas/Fas ligand-dependent mechanism. J Immunol 2006;177(9):6540–7. [PubMed: 17056586]

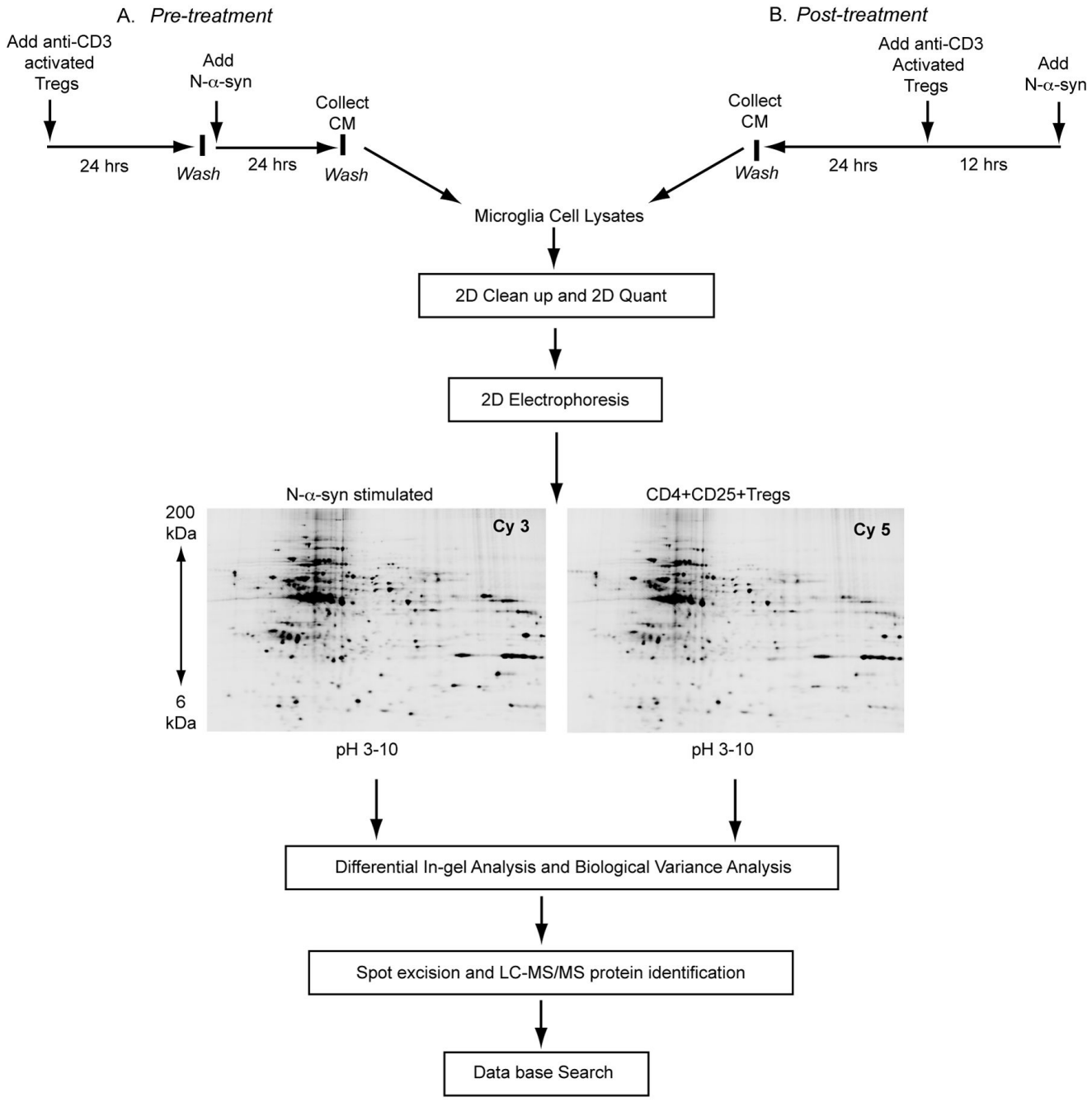

Figure 1.

Experimental design for microglial proteomics protein discovery. Microglia were co-cultured for 24 h with CD4+CD25+ Treg (or Teff) or without as control. Treg (or Teff) were removed from the cultures and the microglia stimulated with aggregated N-α-syn for 24 h [pre-treatment] to represent asymptomatic disease (A). Alternatively, microglia were stimulated with N-α-syn for 12 h prior to the addition of Treg [post-treatment] to represent more overt disease (B). Twenty-four hours later microglial cell protein lysates were prepared and subjected to 2D electrophoresis. Decyder analysis software was used to match spots and identify expression patterns. Selected protein spots were excised, digested with trypsin and identified by *nano*-LC-

MS/MS peptide sequencing. Database searches were performed using SEQUEST with criteria thresholds set to afford greater than 95% confidence level in peptide identification.

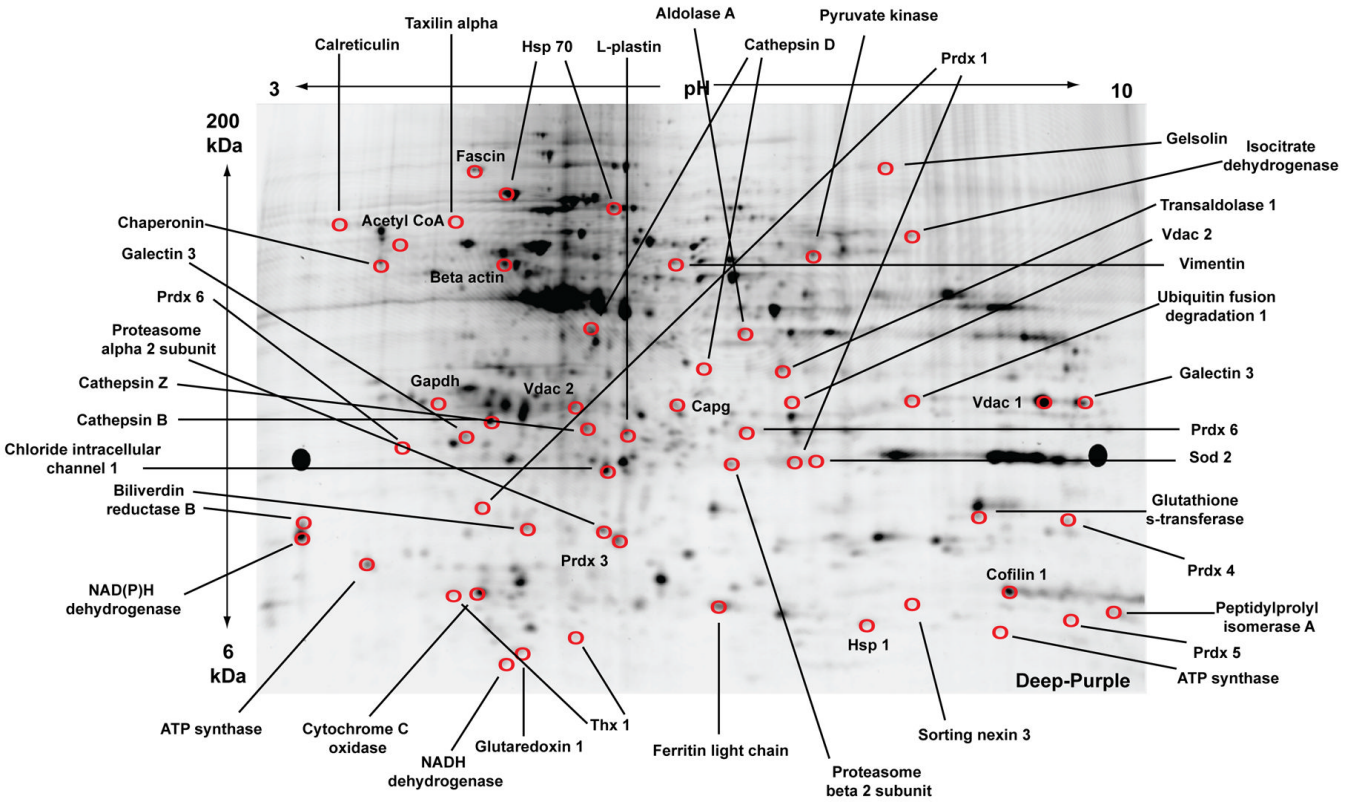

Figure 2.

2D-DIGE of proteins from all experimental groups with matched spots picked for sequencing identifications by *nano*-LC-MS/MS. A representative preparative gel is shown. Equal amounts of protein were pooled from all experimental groups (unstimulated, N-α-syn-stimulated, pre- and post-treatment with Treg or Teff) and replicates for a total concentration of 450 μg. The pooled sample was applied to a pH gradient strip and separated with isoelectric focusing for the first dimension. For the second dimension, the strip was loaded onto a large format gradient gel and separated based on molecular weight. Following electrophoresis, the gel was fixed and post-stained with Deep Purple for positive detection of protein spots. Circled spots identified by BVA using Decyder analysis software were selected for excision. Proteins with the most peptides positively identified within a specific spot are labeled on the gel. (Abbreviations: Prdx, peroxiredoxin; Thx, thioredoxin, Vdac, voltage-dependent anion channel; Sod, superoxide dismutase; Hsp, heat shock protein; Capg, macrophage capping protein; NAD, nicotinamide adenine dinucleotide).

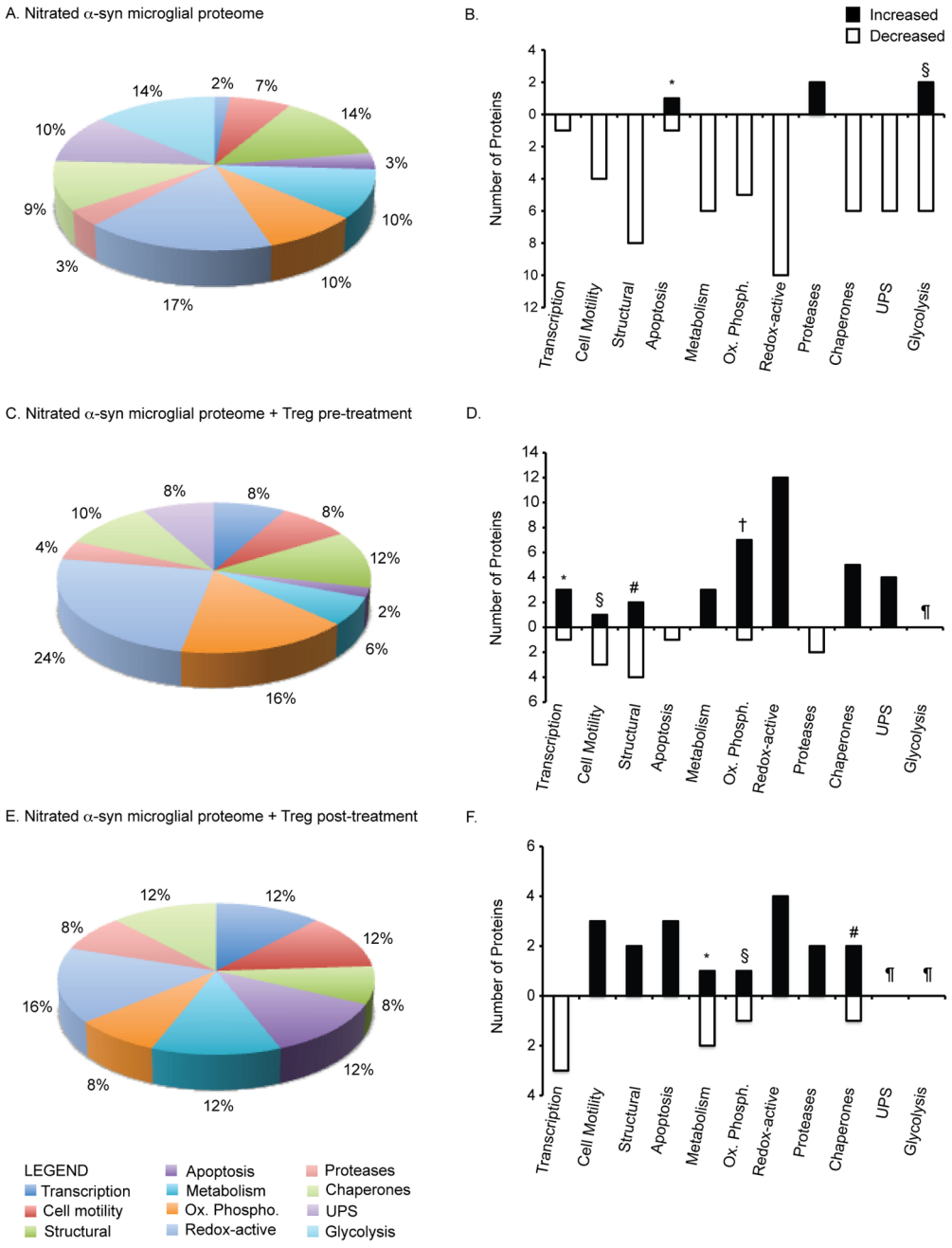

Figure 3.

Classification of proteins modulated by N-α-syn stimulation and Treg treatment. Pie-chart diagrams represent the proportion (%) of proteins within specific categories based on classification and function identified by mass spectrometry. (A) Classification of proteins differentially expressed by microglia in response to N-α-syn stimulation alone. (B) Relative expression of proteins in response to N-α-syn stimulation compared to unstimulated controls. Several proteins within each category showing both increased and decreased proteins were identified including those for apoptosis (*gelsolin increased; nucleoside-diphosphate kinase decreased) and glycolysis (§enolase 3 and lactate dehydrogenase increased; alpha enolase, pyruvated dehydrogenase, pyruvate kinase, and triosphosphate isomerase 1 decreased) (Table

1). (C) Proportion of microglial proteins differentially expressed in response to N-α-syn following Treg pre-treatment and the relative expression trends shown in D. Categories associated with transcription (*VIP-receptor gene repressor protein, TAR DNA binding protein, and Ubiquitin conjugating enzyme E2N increased; MRG-binding protein decreased), cell motility ([§]microtubule associated protein increased; laminin B2, beta actin, and alpha tubulin decreased), structural ([#]Capg and guanine nucleotide exchange factor increased; vimentin, cofilin 1 and 2 decreased), and oxidative phosphorylation ([†]NADH dehydrogenase Fe-S, ATP synthase O subunit, H+-ATP synthase e subunit, and cytochrome c oxidase increased; ATP synthase F0 complex decreased) consisted of both increased and decreased expression of proteins (Table 2). (E) Proportion of microglial proteins differentially expressed in response to N-α-syn following Treg post-treatment and the relative expression trends shown in F. Categories associated with metabolism ([#]phosphoglycerate mutase 1 increased; aldolase 1 and aldehyde dehydrogenase 2 decreased), oxidative phosphorylation ([§]ATP synthase D increased; H+-transporting two-sector ATPase alpha chain decreased), and chaperones ([#]cyclophilin A increased; protein disulfide isomerase decreased) consisted of both increased and decreased expression of proteins (Table 3). ([¶]Proteins within this category were not identified as differentially expressed).

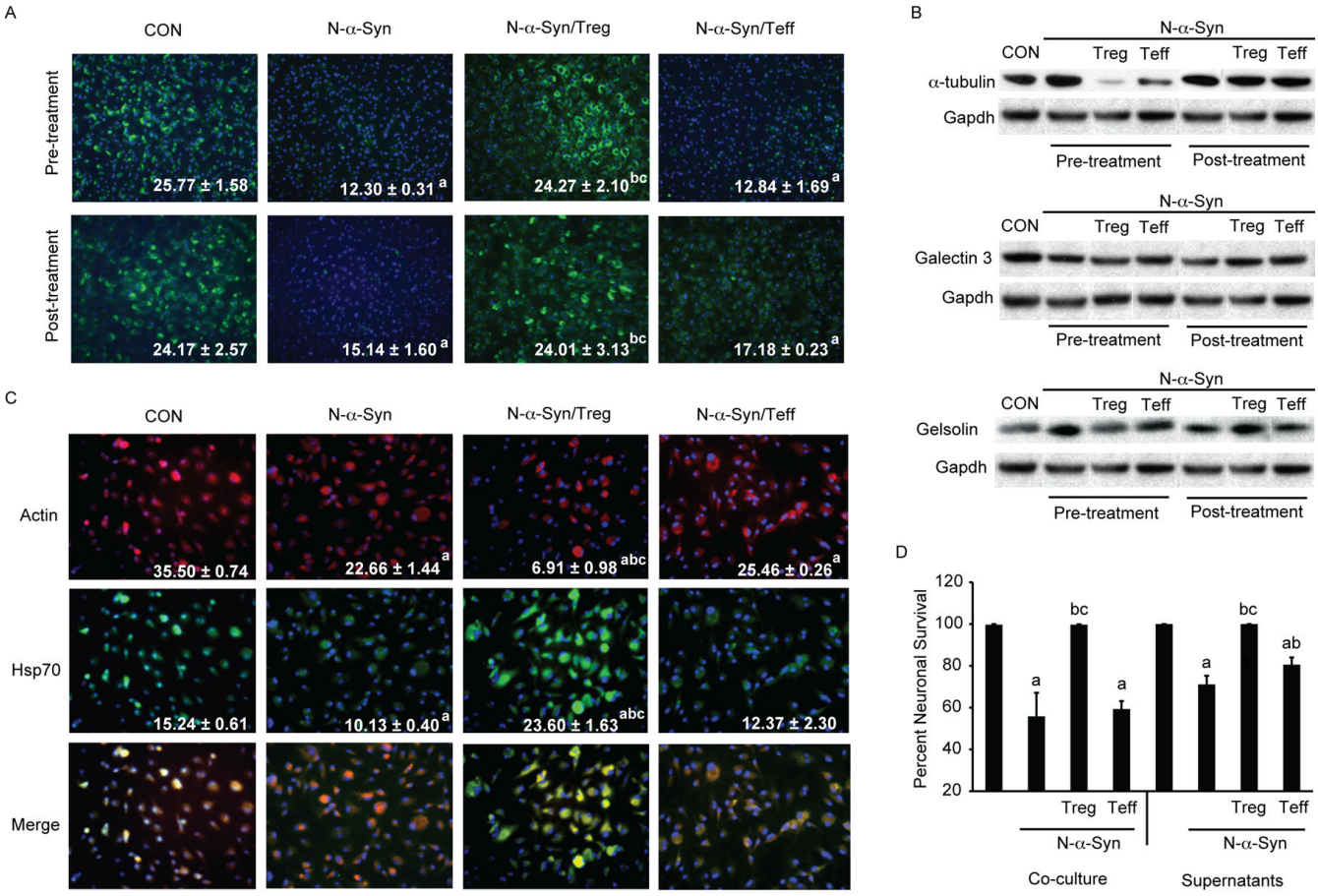

Figure 4.

Treg modulate microglial inflammation to attenuate the neurotoxic phenotype of N-α-syn stimulated microglia. (A) Photomicrographs (20× magnification) of Prx1 expression (green) in microglia treated with media alone (CON), N-α-syn, or cultured with CD4+ T cell subsets following pre-and post-treatment. Values shown are the mean fluorescence intensity (MFI) per field ± SEM. (B) Western blot analysis for α-tubulin, galectin 3 and gelsolin in response to treatment normalized to Gapdh expression within the same blot for comparisons. (C) Photomicrographs (20× magnification) of actin expression (red) or Hsp70 (green) in microglia treated with media alone (CON), N-α-syn, or cultured with CD4+ T cell subsets following pre- and post-treatment. Values shown are the MFI per field ± SEM. (D) Survival of MES23.5 cells after co-culture with N-α-syn stimulated microglia with and without Treg or Teff or after culture with condition media (supernatants) of N-α-syn stimulated microglia treated with either Treg or Teff. Values ± SEM ($P < 0.01$ vs. [a]CON, [b]N-α-syn alone, [c]N-α-syn/Teff).

Table 1

N-α-syn stimulated proteome

Protein ID by LC/MS/MS*	SwissProt†	IPI‡	M.wt.§ (DA)	pI11	Subcellular Location¶	Function#	Peptide**#	DIGE†† Index	P-value‡‡
Heterogeneous nuclear ribonucleoprotein A2/B1 isoform 2	O88569	IPI00622847	37403	8.97	Nucleus	transcription	2	-1.69	
Guanine nucleotide-binding protein	P62880	IPI00162780	37331	5.60	Cytoplasm	GTPase activity	2	-1.5	0.004
Guanine nucleotide-binding protein	Q61011	IPI00116938	37240	5.41	Cytoplasm	GTPase activity	2	-1.5	0.004
Interleukin-6 receptor subunit beta	Q00560	IPI00120155	102452	5.32	Membrane	signal transduction	3	-1.84	0.05
Ubiquitin A-52 residue ribosomal protein fusion	B0LAC2	IPI00138892	8038.2	6.89	Ribosome	protein modification	2	-1.51	0.05
Alpha tubulin	P68369	IPI00110753	50136	4.94	Cytoskeleton	cell motility	2	-2.21	
Beta actin	P60710	IPI00110850	269833	5.82	Cytoskeleton	cell motility	3	-1.5	0.046
Dynein cytoplasmic 1 intermediate chain 2	O88487	IPI00131086	68394	5.16	Cytoskeleton	cell motility	2	-2.21	
Galectin 3	P16110	IPI00131259	27515	8.47	Cytoplasm/nucleus	protein binding, phagocytosis	4	-2.96	
L-plastin	Q61233	IPI00118892	70149	5.2	Cytoskeleton	phagocytosis	2	-1.95	
RuvB-like protein 1	P60122	IPI00133985	50214	6.02	Nucleus	proliferation	5	-1.5	
Voltage-dependent anion channel 2	Q60930	IPI00122547	31733	7.44	Mitochondria	ion transport	6	-1.71	
Voltage-dependent anion channel 3	Q60931	IPI00876341	30753	8.96	Mitochondria	ion transport	19	-1.94	
Vacuolar H+ATPase B2	P62814	IPI00119113	56551	5.57	Membrane	ion transport	6	-1.82	0.04
Voltage-dependent anion-selective channel protein 1 (VDAC-1)	Q60932	IPI00230540	32351	8.55	Membrane/ Mitochondria	ion transport	3	-1.94	
G-protein beta subunit	Q61621	IPI00120716	13533	5.50	Membrane	G-protein signaling	4	-1.5	0.004
Lamin A isoform C2	P48678	IPI00230435	74238	6.54	Nucleus	membrane stabilization	22	-1.67	0.017
Cofilin 1	P18760	IPI00890117	18559	8.22	Cytoskeleton	actin polymerization	3	-2.15	0.02
Cofilin 2	P45591	IPI00266188	18710	7.66	Cytoskeleton	actin polymerization	2	-2.15	0.02
Vimentin	P20152	IPI00227299	53688	5.06	Cytoskeleton	stabilize cytoskeleton	5	-2.35	0.05
Peripherin	P15331	IPI00129527	54268	5.40	Cytoskeleton	cytoskeleton organization	2	-2.35	0.05
Desmin	P31001	IPI00130102	53498	5.21	Cytoskeleton	stabilize cytoskeleton	2	-2.35	0.05
Adenylyl cyclase-associated protein 1 (CAP 1)	P40124	IPI00137331	51575	7.16	Cytoskeleton	cytoskeleton organization	3	-2.39	0.05
Fascin	Q61553	IPI00353563	54508	6.44	Filopodium	actin binding	3	-1.63	
Annexin A2	P07356	IPI00468203	38676	7.55	Secreted	matrix	2	-1.5	
Annexin A10	Q9QZ10	IPI00136659	37301	5.40	Mitochondria	matrix	2	-1.63	0.05
Inner membrane protein, mitochondria	Q8CAQ8	IPI00228150	83900	6.18	Mitochondria	matrix	7	-1.58	

Protein ID by LC/MS/MS*	SwissProt†	IPI‡	M.wt.§ (DA)	pI11	Subcellular Location¶	Function#	Peptide**#	DIGE†† Index	P-value‡‡
Gelsolin	A2AL35	IPI00117167	85942	5.83	Cytoskeleton	apoptosis and inflammation, vesicle transport	8	1.53	0.05
Annexin A1	P10107	IPI00230395	38734	6.97	Cytoplasm	membrane fusion and exocytosis	2	-1.5	
Palmitoyl-protein thioesterase 1	B1B0P8	IPI00881289	19550	8.09	Membrane/ Lysosome	endocytosis/ protein transport	2	-1.5	
Rho GDP dissociation inhibitor (GDI) alpha	Q99PT1	IPI00322312	23407	5.12	Cytoplasm/ membrane	protein binding	9	-2.08	
Cryptochrome 2	Q9R194	IPI00128234	66850	8.66	Cytoplasm/nucleus	protein transport	3	-1.5	0.039
14-3-3 zeta	P63101	IPI00116498	27111	4.73	Mitochondria	protein targeting	5	-2.39	0.05
Ferritin light chain 1	P29391	IPI00762203	20802	5.66	Cytoplasm	iron homeostasis	5	-1.75	0.05
Ferritin heavy chain 1	P09528	IPI00230145	21067	5.53	Cytoplasm	iron homeostasis	3	-1.61	0.02
Acetyl-Coenzyme A acetyltransferase 1	A8XUS5	IPI00228253	41298	7.16	Cytoplasm	metabolism	4	-1.52	
Acetyl-Coenzyme A acyltransferase 2	A8XUT1	IPI00881591	38147	7.63	Cytoplasm	metabolism	2	-1.52	
Aldehyde dehydrogenase, mitochondrial	P47738	IPI00111218	56538	7.53	Mitochondria	metabolism	23	-2.79	
Hexosaminidase B	P20060	IPI00115530	61116	8.28	Lysosome	metabolism	4	-2.79	
Ugp2 protein	Q8R0M2	IPI00279474	55498	6.92	Cytoplasm	metabolism	6	-1.5	0.028
Pyrophosphatase	Q9D819	IPI00110684	32667	5.37	Cytoplasm	metabolism	7	-1.73	
Aldo-keto reductase family 1, member B8	Q3UJW9	IPI00466128	36615	6.90	Cytoplasm/ membrane	catabolism	4	1.6	
Catechol O-methyltransferase	O88587	IPI00759876	29496	5.52	Cytoplasm	catabolism	3	1.51	0.05
Glutamate oxaloacetate transaminase 2, mitochondrial	P05202	IPI00117312	47411	9.13	Mitochondria	catabolism	6	-1.5	0.046
Fatty acid-binding protein	P05201	IPI00230204	46232	6.68	Cytoplasm	catabolism	4	-3.57	0.02
Cathepsin B	P10605	IPI00113517	37280	5.57	Lysosome	thiol protease	4	2.86	0.005
Cathepsin D	P18242	IPI00111013	44954	6.71	Lysosome	acid protease	4	1.62	0.036
Calreticulin	P14211	IPI00123639	47995	4.33	Membrane/ ER	chaperone	6	-4.6	
Calreticulin 3 isoform 1	Q9D9Q6	IPI00113023	44198	5.99	ER	chaperone	2	-2.75	
Chaperonin subunit 6a zeta	Q52KG9	IPI00116281	58076	6.46	Cytoplasm	chaperone	3	-1.67	0.017
HSP 10	Q64433	IPI00263863	10963	7.91	Mitochondria	chaperone	2	-3.29	
HSP 60	P63038	IPI00308885	60955	5.91	Mitochondria	chaperone	17	-2.35	0.05
HSP 70	P63017	IPI00323357	70871	5.37	Cytoplasm	chaperone	17	-2.35	0.05
Proteasome subunit, alpha type 2	P49722	IPI00890001	25926	8.39	Cytoplasm	Ubiquitin-Proteasome system	2	-1.53	0.05
Proteasome subunit, alpha type 3	O70435	IPI00331644	28405	5.29	Cytoplasm/nucleus	Ubiquitin-Proteasome system	6	-2.39	0.05
Proteasome subunit, alpha type 6	Q9QUM9	IPI00131845	27372	6.35	Cytoplasm/nucleus	Ubiquitin-Proteasome system	4	-1.54	

Protein ID by LC/MS/MS[*]	SwissProt[†]	IPI[‡]	M.wt.[§] (DA)	pI[11]	Subcellular Location[¶]	Function[#]	Peptide[**#]	DIGE[††] Index	*P*-value[‡‡]
Proteasome subunit alpha type 7	Q9Z2U0	IPI00131406	27855	8.59	Cytoplasm/nucleus	Ubiquitin-Proteasome system	3	-1.69	0.027
20S proteasome subunit C2	Q9JHS5	IPI00283862	4581.4	8.07	Cytoplasm	Ubiquitin-Proteasome system	2	-1.54	0.05
Ubiquitin-conjugating enzyme E2-25K	P61087	IPI00322440	22407	5.33	Cytoplasm	Ubiquitin-Proteasome system	8	-1.51	0.05
Superoxide dismutase 1, soluble	P08228	IPI00130589	15943	6.02	Cytoplasm/mitochondria	redox	9	-1.54	0.05
Thioredoxin reductase 2	Q9JLT4	IPI00124699	56453	8.72	Mitochondria	redox	2	-1.5	0.028
Biliverdin reductase B (NADPH)	Q923D2	IPI00113996	22197	6.49	Cytoplasm	redox	9	-1.53	0.05
Peroxiredoxin 1	P35700	IPI00121788	22177	8.26	Cytoplasm	redox	2	-1.54	0.05
Peroxiredoxin 4	O08807	IPI00116254	31053	6.67	Cytoplasm	redox	2	-1.69	0.05
Peroxiredoxin 6	O08709	IPI00555059	24871	5.71	Cytoplasm/lysosome	redox	6	-1.59	0.05
Isocitrate dehydrogenase [NADP] cytoplasmic	O88844	IPI00135231	46660	6.48	Cytoplasm	redox	4	-4.43	
Glutaredoxin 1	Q9QUH0	IPI00331528	11871	8.68	Cytoplasm	redox	4	-1.72	
Glutathione reductase 1 precursor	P47791	IPI00111359	53663	8.19	Cytoplasm/mitochondria	redox	2	-1.5	0.028
Alpha enolase	P17182	IPI00462072	47141	6.37	Cytoplasm/ membrane	glycolysis	3	-2.08	
Enolase 3, beta	P21550	IPI00228548	47025	6.73	Cytoplasm	glycolysis	2	1.56	
Lactate dehydrogenase A	P06151	IPI00319994	36499	7.61	Cytoplasm	glycolysis	12	1.63	
Pyruvate dehydrogenase (lipoamide) beta	Q9D051	IPI00132042	38937	6.41	Mitochondria	glycolysis	8	-1.5	0.004
Pyruvate dehydrogenase E1 alpha 1	P35486	IPI00337893	43232	8.49	Mitochondria	glycolysis	2	-2.66	
Pyruvate kinase M	P52480	IPI00407130	57845	7.17	Mitochondria	glycolysis	2	-2.08	
Triosephosphate isomerase 1	P17751	IPI00467833	26713	6.90	Cytoplasm	glycolysis	2	-1.53	0.05
Malate dehydrogenase	P14152	IPI00336324	36511	6.16	Cytoplasm	TCA cycle	2	-1.94	
Dihydrolipoamide dehydrogenase	O08749	IPI00874456	54272	7.99	Mitochondria	oxidoreductase	2	-1.63	
Nucleoside-diphosphate kinase	Q5NC82	IPI00127417	17363	6.97	Mitochondria	cell survival/apoptosis	4	-5.68	
ATP synthase, H+ transporting mitochondrial F1 complex, delta subunit	Q4FK74	IPI00453777	17600	5.03	Mitochondria (Complex V)	oxidative phosphorylation	3	-1.84	
ATP synthase, H+ transporting, mitochondrial F0 complex, subunit d	B1ASE1	IPI00230507	18749	5.52	Mitochondria (Complex V)	oxidative phosphorylation	2	-1.51	0.05
ATP synthase, H+ transporting, mitochondrial F0 complex, subunit b	Q5I0W0	IPI00341282	28949	9.11	Mitochondria (Complex V)	oxidative phosphorylation	3	-2.66	
ATP synthase, H+ transporting, mitochondrial F1F0 complex, subunit e	Q5EBI8	IPI00111770	8236.5	7.99	Mitochondria (Complex V)	oxidative phosphorylation	20	-1.88	0.011
Electron transferring flavoprotein, alpha polypeptide	B1B1B4	IPI00116753	35009	8.62	Mitochondria	electron transport	2	-1.71	

[*] The CID spectra were compared against those of the EMBL nonredundant protein database by using SEQUEST (ThermoElectron, San Jose, CA). After filtering the results based on cross correlation Xcorr (cutoffs of 2.0 for [M+ H]1+, 2.5 for [M + 2H]2+, and 3.0 for [M + 3H]3+), peptides with scores greater than 3000 and meeting delta cross-correlation scores (ΔCn) > 0.3, and fragment ion numbers > 60% were deemed valid by these SEQUEST criteria thresholds, which have been determined to afford greater than 95% confidence level in peptide identification.

[†] SwissProt accession number (accessible at http://ca.expasy.org/sprot/).

[‡] International Protein Index (IPI) (accessible at http://www.ebi.ac.uk/IPI/).

[§] Theoretical molecular mass for the primary translation product calculated from protein DNA sequences.

[11] Theoretical isoelectric point.

[¶] Postulated subcellular location (accessible at http://locate.imb.ug.edu.au).

[#] Postulated cellular function (accessible at http://ca.expasy.org/sprot/).

[**] Number of different peptides identified for each protein.

[††] Fold changes of proteins in N-α-syn stimulated microglial lysates versus unstimulated microglial lysates. Negative DIGE index indicates decreased expression in N-α-syn stimulated microglia relative to controls.

[‡‡] P-values as determined by Biological Variation Analysis by one-way ANOVA for pair-wise comparison between treatments.

Table 2

Modulation of the N-α-syn microglial proteome by Treg pretreatment

LC/MS/MS* Protein ID by	SwissProt†	IPI‡	M.wt.§ (DA)	pI[11]	Subcellular Location¶	Function#	Peptide#**	DIGE†† Index	*P*-value‡‡
VIP-receptor-gene repressor protein	O88461	IPI00209665	72972	9.57	Nucleus	transcription	2	1.5	0.0011
TAR DNA binding protein	Q921F2	IPI00121758	44548	6.26	Nucleus	transcription	2	1.52	0.003
MRG-binding protein	Q9DAT2	IPI00119018	23888	4.87	Nucleus	transcription	2	-3.79	<0.0001
Ubiquitin conjugating enzyme E2N	P61089	IPI00165854	17138	6.13	Nucleus	transcription	3	2.15	0.0076
Eukaryotic translation initiation factor 3, subunit H	Q91WK2	IPI00128202	39832	6.19	Nucleus	translation	2	-1.52	0.0037
Laminin B2	Q61292	IPI00119065	196352	6.28	Secreted	cell motility	2	-1.51	0.0038
Beta actin	P60710	IPI00110850	269833	5.82	Cytoskeleton	cell motility	5	-2.09	0.0008
Alpha-tubulin	P68369	IPI00110753	50136	4.94	Cytoskeleton	cell motility	2	-1.51	0.0038
Microtubule-associated protein, RP/EB family, member 1	Q7TN34	IPI00117896	29885	5.12	Cytoskeleton	cell motility	9	1.5	0.0011
Chloride intracellular channel 1	Q9Z1Q5	IPI00130344	27013	5.09	Cytoplasm	ion channel	6	1.55	0.003
Voltage-dependent anion channel 2	Q60930	IPI00122547	31733	7.44	Mitochondria	ion channel	3	1.53	0.005
Voltage-dependent anion channel 1	Q60932	IPI00122549	32351	8.55	Mitochondria	ion channel	5	1.88	<0.0001
Vimentin	P20152	IPI00227299	53688	5.06	Cytoskeleton	stabilize cytoskeleton	6	-1.63	0.0002
Cofilin 1	P18760	IPI00890117	18559	8.22	Cytoskeleton	actin polymerization	3	-1.61	0.0022
Cofilin 2	P45591	IPI00266188	18710	7.66	Cytoskeleton	actin polymerization	2	-1.5	0.05
Macrophage capping protein (CAPG)	P24452	IPI00136906	39240	6.73	Cytoplasm	inhibits actin polymerization	9	1.82	0.036
Guanine nucleotide exchange factor GEFT	Q9CWR0	IPI00109434	68262	5.19	Cytoplasm	actin reorganization	4	2.7	<0.0001
Gelsolin	A2AL35	IPI00117167	85942	5.83	Cytoskeleton	apoptosis and inflammation, vesicle transport	5	-2.48	0.0002
Galectin 3	P16110	IPI00131259	27515	8.47	Cytoplasm/nucleus	protein binding, phagocytosis	26	-1.68	0.0016
Early endosome antigen 1	Q8BL66	IPI00453776	160915	5.99	Cytoplasm	endosomal trafficking	8	-2.41	<0.0001
Annexin A1	P10107	IPI00230395	38734	6.97	Cytoplasm	membrane fusion and exocytosis	3	1.53	0.0047
Annexin A4	P97429	IPI00353727	35990	5.43	Cytoplasm	membrane fusion and exocytosis	18	1.5	0.0011
Nestin	Q6P5H2	IPI00453692	207124	4.3	Cytoplasm	protein trafficking	2	1.51	0.023
cAMP-dependent protein kinase	P05132	IPI00227900	40571	8.84	Cytoplasm	protein trafficking	5	-1.59	0.05
Non-specific lipid transfer protein	P32020	IPI00134131	59126	7.16	Cytoplasm	lipid protein transfer	3	4.42	<0.0001
Glycolipid transfer protein	Q9JL62	IPI00229718	23690	6.9	Cytoplasm	lipid protein transfer	2	1.55	0.003

LC/MS/MS[*] Protein ID by	SwissProt[†]	IPI[‡]	M.wt.[§] (DA)	pI[11]	Subcellular Location[¶]	Function[#]	Peptide[#**]	DIGE[††] Index	*P*-value[‡‡]
Peptide chain release factor 1	Q8BWY3	IPI00312468	49031	5.51	Cytoplasm	termination of peptide synthesis	3	1.71	0.034
L-Plastin	Q61233	IPI00118892	70149	5.2	Cytoskeleton	phagocytosis	25	2.1	0.0029
Ferritin light chain 1	P29391	IPI00762203	20802	5.66	Cytoplasm	iron homeostasis	2	1.51	0.023
Ferritin heavy chain	P09528	IPI00230145	21067	5.53	Cytoplasm	iron homeostasis	8	-1.54	0.0033
Transaldolase 1	Q93092	IPI00124692	37387	6.57	Cytoplasm	metabolism	7	1.71	0.034
Hypoxanthine guanine phosphoribosyl transferase 1	P00493	IPI00284806	24570	6.21	Cytoplasm	metabolism	4	2.33	<0.0001
Sterol carrier protein 2	A2APS3	IPI00134131	59126	7.16	Mitochondria	metabolism	9	4.42	<0.0001
Aconitate hydratase	Q99KI0	IPI00116074	85464	8.08	Mitochondria	enzyme	2	1.51	0.023
Lysosomal alpha-mannosidase precursor	O09159	IPI00381303	114604	8.3	Lysosome	catabolism	3	2.59	<0.0001
Contrapsin	P07759	IPI00131830	46880	5.05	Secreted	protease inhibitor	3	6.56	<0.0001
Calpastatin	P51125	IPI00409176	84922	5.37	Cytoplasm	protease inhibitor	2	-1.86	0.0004
Cathepsin B	P10605	IPI00113517	37280	5.57	Lysosome	thiol protease	15	-3.34	<0.0001
Cathepsin D	P18242	IPI00111013	44954	6.71	Lysosome	acid protease	5	-2.09	0.0008
Cathepsin Z	Q9R1T3	IPI00207663	34194	6.74	Cytoplasm/Secreted	peptidase	2	1.5	0.0011
SDF2 like protein 1	Q9ESP1	IPI00227657	23648.34	6.92	ER	stress response	3	2.59	0.0067
Calreticulin	P14211	IPI00123639	47995	4.33	Membrane/ ER	chaperone	20	2.32	<0.0001
HSP 10	Q64433	IPI00263863	10962.7	7.91	Mitochondria	chaperone	5	1.52	0.0025
HSP 70	P63017	IPI00323357	70871	5.37	Cytoplasm	chaperone	3	1.59	0.0097
HSP 90	Q80Y52	IPI00330804	84788	4.93	Cytoplasm	chaperone	2	2.09	0.0004
Proteasome subunit beta type-2	Q9R1P3	IPI00128945	22906	6.52	Cytoplasm	Ubiquitin-Proteasome system	4	2.59	<0.0001
Proteasome (prosome, macropain) subunit, alpha type 2	P49722	IPI00890001	25926	8.39	Cytoplasm	Ubiquitin-Proteasome system	7	6.56	<0.0001
Ubiquitin specific protease 19	Q3UJD6	IPI00420483	150549	5.99	Cytoplasm	Ubiquitin-Proteasome system	2	4.42	<0.0001
Ubiquitin fusion degradation	P70362	IPI00656165	34484	6.97	Cytoplasm/ ER	Ubiquitin-Proteasome system	2	1.52	0.0037
Immune costimulatory protein B7-H4	Q7TSP5	IPI00169522	30875	5.69	Membrane	immune response	2	-1.59	0.05
Interferon-alpha/beta receptor alpha chain precursor	P33896	IPI00115420	65777	5.37	Membrane	immune response	2	3.29	<0.0001
Interferon-induced GTP-binding protein	Q01514	IPI00124675	67712	5.41	Membrane	immune response	2	-1.83	0.0011
Peroxiredoxin 1	P35700	IPI00121788	22177	8.26	Cytoplasm	redox	7	2.59	<0.0001
Peroxiredoxin 3	Q9Z0V6	IPI00208215	28295	7.14	Mitochondria	redox	7	2.7	<0.0001
Peroxiredoxin 4	O08807	IPI00116254	31053	6.67	Cytoplasm	redox	8	2.33	<0.0001

LC/MS/MS* Protein ID by	SwissProt†	IPI‡	M.wt.§ (DA)	pI11	Subcellular Location¶	Function#	Peptide#**	DIGE†† Index	*P*-value‡‡
Peroxiredoxin 5	P99029	IPI00129517	21897	9.1	Mitochondria	redox	3	2.43	<0.0001
Peroxiredoxin 6	O08709	IPI00555059	24871	5.71	Cytoplasm/lysosome	redox	4	1.7	0.05
Superoxide dismutase 1 [Cu-Zn]	P08228	IPI00130589	15943	6.02	Cytoplasm/mitochondria	redox	2	1.6	0.05
Superoxide dismutase 2 [Mn]	P09671	IPI00109109	24603	8.8	Mitochondria	redox	2	1.71	<0.0001
Glutaredoxin 1	Q9QUH0	IPI00331528	11871	8.68	Cytoplasm	redox	2	1.82	<0.0001
Biliverdin reductase B (NADPH)	Q923D2	IPI00113996	22197	6.49	Cytoplasm	redox	13	6.56	<0.0001
Oxidation resistance 1	Q4KMM3	IPI00277552	83016	4.9	Mitochondria	redox	2	1.51	0.05
Thioredoxin 1	P10639	IPI00226993	11675	4.8	Mitochondria	redox	3	3.36	<0.0001
Catalase	P24270	IPI00312058	59765	7.72	Mitochondria	redox	2	2.13	0.014
Prohibitin	P67778	IPI00133440	29820	5.57	Mitochondria	respiration activity	2	2.7	<0.0001
NADH dehydrogenase (ubiquinone) Fe-S protein-2	Q923F9	IPI00229008	18518	9.9	Mitochondria (Complex I)	oxidative phosphorylation	3	2.94	0.0012
Mitochondrial ATP synthase, O subunit	Q9DB20	IPI00118986	23364	10	Mitochondria (Complex V)	oxidative phosphorylation	3	2.59	0.0067
H(+)-ATP synthase subunit e	P56382	IPI00230241	5838	10.01	Mitochondria (Complex V)	oxidative phosphorylation	2	1.52	0.0025
ATP synthase, H+ transporting, mitochondrial F1F0 complex, subunit e	Q5EBI8	IPI00111770	8237	7.99	Mitochondria (Complex V)	oxidative phosphorylation	4	1.52	0.0025
ATP synthase, H+ transporting, mitochondrial F0 complex, subunit d	B1ASE1	IPI00230507	18749	5.52	Mitochondria (Complex V)	oxidative phosphorylation	21	-1.83	0.0011
Cytochrome c oxidase, subunit Va	P12787	IPI00120719	16101	6.08	Mitochondria (Complex IV)	oxidative phosphorylation	4	2.65	0.014
Cytochrome c oxidase, subunit VIb polypeptide 1	P56391	IPI00225390	10071	8.96	Mitochondria (Complex IV)	oxidative phosphorylation	2	2	0.0012

*The CID spectra were compared against those of the EMBL nonredundant protein database by using SEQUEST (ThermoElectron, San Jose, CA). After filtering the results based on cross correlation Xcorr (cutoffs of 2.0 for [M+ H]1+, 2.5 for [M + 2H]2+, and 3.0 for [M + 3H]3+), peptides with scores greater than 3000 and meeting delta cross-correlation scores (ΔCn) > 0.3, and fragment ion numbers > 60% were deemed valid by these SEQUEST criteria thresholds, which have been determined to afford greater than 95% confidence level in peptide identification.

†SwissProt accession number (accessible at http://ca.expasy.org/sprot/).

‡International Protein Index (IPI) (accessible at http://www.ebi.ac.uk/IPI/).

§Theoretical molecular mass for the primary translation product calculated from protein DNA sequences.

11Theoretical isoelectric point.

¶Postulated subcellular location (accessible at http://locate.imb.ug.edu.au).

#Postulated cellular function (accessible at http://ca.expasy.org/sprot/).

[**] Number of different peptides identified for each protein.

[††] Fold changes of proteins in Treg pre-treated microglia versus N-α-syn alone stimulated microglial lysates. Negative DIGE index indicates decreased expression in N-α-syn stimulated microglia relative to controls.

[‡‡] P-values as determined by Biological Variation Analysis by one-way ANOVA for pair-wise comparison between treatments.

Table 3

Modulation of the N-α-syn microglial proteome by Treg post-treatment

LC/MS/MS* Protein ID by	SwissProt†	IPI‡	M.wt.§ (DA)	p11	Subcellular Location¶	Function#	Peptide#**	DIGE†† Index	*P*-value‡‡
Histone H4	P62806	IPI00407339	11367	11.21	Nucleus	nucleosome component	3	-1.56	0.021
Histone H2B	Q64475	IPI00554853	13592	10.31	Nucleus	nucleosome component	2	-2.28	
Heterogeneous nuclear ribonucleoprotein A3 (hnRNP A3)	Q8BG05	IPI00269661	39652	8.46	Nucleus	cytoplasmic trafficking of RNA	5	-1.62	
GTP-binding nuclear protein Ran	P62827	IPI00134621	24423	7.19	Nucleus/Cytoplasm	GTPase activity	5	1.35	0.033
Rho GTPase-activating protein 1	Q5FWK3	IPI00404970	50411	5.97	Membrane	GTPase activity	2	-1.75	0.05
Rho GDP-dissociation inhibitor	Q99PT1	IPI00322312	23407	5.12	Cytoplasm	GTPase activity	2	1.48	0.046
Guanine nucleotide-binding protein subunit beta-2	P62880	IPI00162780	37331	7.06	Membrane	signaling	14	1.32	0.018
Stathmin	P54227	IPI00551236	17274	5.77	Cytoplasm	cell motility	3	1.52	0.0024
Beta-actin	P60710	IPI00110850	41737	5.78	Cytoplasm	cell motility	7	1.53	0.015
Gamma-actin	P63260	IPI00874482	41793	5.56	Cytoplasm/Cytoskeleton	cell motility	9	1.54	
Cofilin-1	P18760	IPI00890117	18560	8.22	Cytoplasm	actin polymerization	2	1.63	0.0065
Brain acid soluble protein 1	Q91XV3	IPI00129519	22087	4.5	Membrane	nurite outgrowth	9	1.55	
Gelsolin	A2AL35	IPI00117167	85942	5.83	Cytoskeleton	apoptosis and inflammation, vesicle transport	7	1.73	0.004
Galectin-3	P16110	IPI00131259	27515	8.5	Nucleus	protein binding, phagocytosis	7	1.65	0.067
Cyclophilin A	P17742	IPI00554989	17971	7.74	Cytoplasm	protein folding	6	1.48	0.05
Protein disulfide isomerase	Q8BXZ1	IPI00453798	51848	5.02	ER	protein folding	18	-1.53	
L-Plastin	Q61233	IPI00118892	70149	5.21	Cytoplasm	Phagocytosis	17	-1.53	
Ferritin heavy chain	P09528	IPI00230145	21067	5.53	Cytoplasm	iron homeostasis	2	1.50	0.0072
Ferritin Light Chain 1	P29391	IPI00762203	20802	5.66	Cytoplasm	iron homeostasis	2	1.5	0.0072
Leupaxin	Q8R355	IPI00387515	43460	5.88	Cytoplasm	zinc ion binding	2	1.4	0.0021
Aldolase I	P05064	IPI00221402	39356	8.31	Cytoplasm	metabolism	4	-2.16	
Aldehyde dehydrogenase 2	Q3TVM2	IPI00111218	56596	7.03	Mitochondria	metabolism	4	-1.75	0.05
Phosphoglycerate mutase 1	Q9DBJ1	IPI00457898	28832	6.75	Cytoplasm	metabolism	8	1.37	0.044
Transmembrane glycoprotein NMB (Dendritic cell-associated transmembrane protein)	Q99P91	IPI00311808	63675	7.88	Membrane	enzyme	2	-3.50	0.0089
Alpha-enolase	P17182	IPI00462072	47141	6.36	Cytoplasm	enzyme	9	1.40	0.0021
Beta enolase	P21550	IPI00228548	47025	6.73	Cytoplasm	enzyme	3	1.4	0.0021

LC/MS/MS* Protein ID by	SwissProt†	IPI‡	M.wt.§ (DA)	p11	Subcellular Location¶	Function#	Peptide#**	DIGE†† Index	*P*-value‡‡
S-formylglutathione hydrolase	Q9R0P3	IPI00109142	31320	6.70	Cytoplasm	enzyme	5	1.49	0.0068
Peptidylprolyl isomerase A	Q8CEC6	IPI00229025	73431	6.58	Cytoplasm	enzyme	6	1.48	0.05
Malate dehydrogenase, cytosolic	P14152	IPI00336324	36511	6.16	Cytoplasm	enzyme	2	1.49	0.0068
Nucleoside diphosphate kinase	Q9WV84	IPI00125448	20549	9.21	Mitochondria	enzyme	5	1.48	0.05
Phosphoglycerate kinase 1	P09411	IPI00555069	44540	8.02	Cytoplasm	enzyme	3	1.63	0.0065
Adenylosuccinate synthase	P28650	IPI00123190	50254	8.57	Cytoplasm/Membrane	enzyme	2	-1.74	
Cathepsin B precursor	P10605	IPI00113517	37280	5.57	Lysosome	thiol protease	7	1.6	0.022
Cathepsin D precursor	P18242	IPI00111013	44954	6.71	Lysosome	acid protease	2	1.63	0.0065
Vacuolar proton pump subunit E 1	P50518	IPI00119115	26157	8.44	Cytoplasm	proton pump for acidification of intracellular compartments	8	-2.08	
Beta-N-acetylhexosaminidase	P29416	IPI00125522	60599	6.09	Lysosome	protein degradation	2	-1.75	0.05
Peroxiredoxin-1	P35700	IPI00121788	22176	8.26	Cytoplasm	redox	6	1.38	0.022
Peroxiredoxin-5	P99029	IPI00129517	21897	9.1	Mitochondria/Cytoplasm	redox	6	1.46	0.003
Superoxide dismutase [Cu-Zn]	P08228	IPI00130589	15943	6.03	Cytoplasm	redox	4	1.51	0.048
Vat1	Q62465	IPI00126072	43097	5.95	Membrane	redox	15	1.4	0.0021
H+ transporting two-sector ATPase alpha chain	Q03265	IPI00130280	59753	9.22	Mitochondria (Complex V)	oxidative phosphorylation	18	-1.75	0.048
ATP synthase D chain, mitochondrial	Q9DCX2	IPI00230507	18250	5.52	Mitochondria (Complex V)	oxidative phosphorylation	2	1.5	0.0072
Translation elongation factor 1	Q9D1M4	IPI00133928	19859	8.6	Nucleus/Cytoplasm	DNA damage response	2	-1.74	
Apoptosis-associated speck-like protein containing a CARD	Q9EPB4	IPI00109709	21459	5.03	Cytoplasm	caspase-mediated apoptosis	5	1.51	

*The CID spectra were compared against those of the EMBL nonredundant protein database by using SEQUEST (ThermoElectron, San Jose, CA). After filtering the results based on cross correlation Xcorr (cutoffs of 2.0 for [M+ H]1+, 2.5 for [M + 2H]2+, and 3.0 for [M + 3H]3+), peptides with scores greater than 3000 and meeting delta cross-correlation scores (ΔCn) > 0.3, and fragment ion numbers > 60% were deemed valid by these SEQUEST criteria thresholds, which have been determined to afford greater than 95% confidence level in peptide identification.

†SwissProt accession number (accessible at http://ca.expasy.org/sprot/).

‡International Protein Index (IPI) (accessible at http://www.ebi.ac.uk/IPI/).

§Theoretical molecular mass for the primary translation product calculated from protein DNA sequences.

11Theoretical isoelectric point.

¶Postulated subcellular location (accessible at http://locate.imb.ug.edu.au).

[#] Postulated cellular function (accessible at http://ca.expasy.org/sprot/).

[**] Number of different peptides identified for each protein.

[††] Fold changes of proteins in Treg-post-treated microglia versus N-α-syn alone stimulated microglial lysates. Negative DIGE index indicates decreased expression in N-α-syn stimulated microglia relative to controls.

[‡‡] P-values as determined by Biological Variation Analysis by one-way ANOVA for pair-wise comparison between treatments.